

PURDUE UNIVERSITY
RESEARCH REACTOR
LICENSE NO. R-87
DOCKET NO. 50-182

SAFETY ANALYSIS REPORT
FOR
THE CONVERSION OF THE PURDUE
UNIVERSITY RESEARCH
REACTOR FROM HEU TO LEU FUEL

REDACTED VERSION

SECURITY-RELATED INFORMATION REMOVED

REDACTED TEXT AND FIGURES BLACKED OUT OR DENOTED BY BRACKETS

**SAFETY ANALYSIS REPORT
FOR
THE CONVERSION OF THE PURDUE UNIVERSITY RESEARCH
REACTOR FROM HEU TO LEU FUEL**

**DOCKET NUMBER 50-182
FACILITY LICENSE NO. R-87**

**SUBMITIAL REPORT
Documentation of Analyses of Conversion
of Purdue University Research Reactor
from HEU to LEU Fuel**

**Submitted By:
Jere Jenkins, Director of Radiation Laboratories
Ed Merritt, Asst. Director of Radiation Laboratories/Reactor Supervisor**

**Purdue University Research Reactor
School of Nuclear Engineering
College of Engineering
Purdue University
West Lafayette, IN**

July 2006

TABLE OF CONTENTS

TABLE OF CONTENTS.....	I
LIST OF TABLES	IV
LIST OF FIGURES.....	VI
1 GENERAL DESCRIPTION OF THE FACILITY	1
1.1 Introduction	1
1.2 Summary and Conclusions of Principal Safety Considerations.....	1
1.3 Summary of Reactor Facility Changes.....	1
1.4 Summary of Operating License, Technical Specifications, and Procedural Changes	1
1.5 Comparison With Similar Facilities Already Converted	2
2 SITE CHARACTERISTICS	2
3 DESIGN OF STRUCTURES, SYSTEMS AND COMPONENTS.....	2
4 REACTOR DESCRIPTION	2
4.1 Reactor Facility	4
4.2 Reactor Core.....	6
4.2.1 Fuel Elements.....	8
4.2.2 Control Rods.....	13
4.2.3 Neutron Reflector.....	13
4.2.4 Neutron Source Holder	13
4.2.5 In-Core Experimental Facilities	13
4.2.6 Reactor Materials.....	14
4.3 Reactor Tank and Biological Shield	14
4.4 Core Support Structure	14
4.5 Dynamic Design.....	14
4.5.1 Control Rod Worths and Excess Reactivity	22
4.5.2 Shutdown Margin.....	25
4.5.3 Other Core Physics Parameters	26
4.5.4 Operating Conditions	36
4.6 Functional Design of Reactivity Control Systems.....	53
4.7 Thermal Hydraulic Characteristics	53
4.7.1 NATCON Code Description	53
4.7.2 Fuel Element and Fuel Assembly Geometry.....	53
4.7.3 Thermal Hydraulic Analysis Results	59

5	REACTOR COOLANT SYSTEM	62
6	ENGINEERED SAFETY FEATURES	63
7	INSTRUMENTATION AND CONTROL SYSTEMS	63
8	ELECTRICAL POWER SYSTEMS	63
9	AUXILIARY SYSTEMS	63
9.1	Systems Summary	63
9.2	Ventilation System	63
9.3	Heating and Air Conditioning Systems.....	63
9.4	Fuel Element Handling and Storage	63
9.5	Other Auxiliary Systems.....	64
10	EXPERIMENTAL FACILITIES AND UTILIZATION	64
11	RADIATION PROTECTION PROGRAMS AND WASTE MANAGEMENT	64
12	CONDUCT OF OPERATIONS	65
12.1	Organization and Staff Qualification.....	65
12.2	Procedures.....	65
12.3	Operator Training and Requalification	65
12.4	Emergency Plan.....	65
12.5	Physical Security Plan	65
12.6	Reload and Startup Plan	65
13	ACCIDENT ANALYSIS.....	66
13.1	Maximum Hypothetical Accident.....	66
13.2	Rapid Addition of Reactivity Accident	66
13.3	Reduction in Cooling Accidents	67
13.4	Other Accidents	68
14	TECHNICAL SPECIFICATIONS.....	68
15	OTHER LICENSE CONSIDERATIONS	73
15.1	Prior Utilization of Reactor Components	73
15.2	License Conditions.....	73
15.3	Decommissioning.....	73
APPENDIX 1: NATCON DOCUMENTATION.....		74
	NATCON Code Running Instructions (July 22, 2006).....	74
	2. Hot Channel Factors in the NATCON Code Version 2.0	76

APPENDIX 2: NEW CORE LOADING PROCEDURE (DRAFT) 89
REFERENCES..... 100

LIST OF TABLES

Table 4-1: Summary of Key Nominal Design Parameters of HEU (current) and LEU (Expected) Cores.....	5
Table 4-2: Summary of Key Reactor Physics and Safety Parameters for the HEU (current) and LEU (Expected) Cores	6
Table 4-3: Characteristics of the HEU and LEU Fuel Plates	9
Table 4-4: Composition of HEU and LEU Fuel.....	14
Table 4-5: Material compositions used in HEU core model.....	15
Table 4-6: Calculated and Measured excess reactivity for fresh HEU core.....	16
Table 4-7: Comparison of calculated to measured critical rod positions for HEU core ...	16
Table 4-8: Comparison of measured and calculated control rod worths for HEU core ...	17
Table 4-9: Representation of HEU and LEU fuel plates.	18
Table 4-10: Comparison of HEU and LEU calculated control rod worths.	22
Table 4-11: Comparison of maximum reactivity insertion rates for HEU and LEU cores	25
Table 4-12: Comparison of shutdown margins for HEU and LEU cores.....	26
Table 4-13: Comparison of other core physics parameters for HEU and LEU cores	29
Table 4-14: Water and Fuel Non-Isothermal Temperature Coefficients for PUR-1 HEU Core (Void coefficients are Shown in Units of $\Delta\rho/^\circ\text{C}$ and $\Delta\rho/\%\text{void}$).....	32
Table 4-15: Water and Fuel Non-Isothermal Temperature Coefficients for PUR-1 LEU Core (Void coefficients are Shown in Units of $\Delta\rho/^\circ\text{C}$ and $\Delta\rho/\%\text{void}$).....	36
Table 4-16: PUR-1 HEU Core Heating Tally Results for Critical Position 3.....	39
Table 4-17: Plate Power Computed from Heating Tallies in Bundles 4-4 and 3-3 in PUR-1 HEU Core.	40
Table 4-18: Axial Heating Profile for Plate 262 of Assembly 4-4 with Critical Position 3 ("50-50-50").	42
Table 4-19: LEU Bundle Powers Predicted by f7 and f6 Tallies in MCNP.....	47
Table 4-20: Plate Power (W) Computed from Heating Tallies in Bundles 4-4, 3-3 and 3-4 in PUR-1 LEU Core with 190 Fuel Plates.	48
Table 4-21: Axial and Radial Heating Profile (f6:n,p Tally) for LEU Plate 1348 of Bundle 4-4 with Critical Position 1.	51
Table 4-22: Axial and Radial Heating Profile (f6:n,p Tally for LEU Plate 1215 of Bundle 3-4 with Critical Position 1.	52
Table 4-23: Channel Types and Thickness in PUR-1 Assemblies	56
Table 4-24: Model Dimensions for the HEU and LEU T-H Models.....	57
Table 4-25: Hot Channel Factors for the HEU Core	58
Table 4-26: Hot Channel Factors for the LEU core	59
Table 4-27: ONB Powers for HEU and LEU Cores	60
Table 4-28: 1 kW Operating Conditions for PUR-1 as Determined by NATCON	60
Table 4-29: Key Power Levels for Reactor Operation and LSSS for PUR-1	61

Table 4-30: Power Levels at the Onset of Nucleate Boiling for HEU and LEU Cores. ... 61
Table 13-1: Transient Results for Rapid Insertion of 0.3% $\Delta k/k$ for PUR-1. 67
Table 13-2: Transient Results for Slow Insertion of 0.04% $\Delta k/k/s$ for PUR-1. 68

LIST OF FIGURES

Figure 4-1: PUR-1 Pool Layout	3
Figure 4-2: PUR-1 Grid Plate	7
Figure 4-3: HEU fuel assembly can with nozzle.....	8
Figure 4-4: HEU Fuel Element	10
Figure 4-5: LEU Fuel element	10
Figure 4-6: HEU Control Fuel Element.....	11
Figure 4-7: LEU Control Fuel Elementy.....	11
Figure 4-8: HEU Standard Fuel Assembly	12
Figure 4-9: LEU Standard Fuel Assembly	12
Figure 4-10: HEU plate in X-Z plane	18
Figure 4-11: HEU plate in Y-Z plane	18
Figure 4-12: LEU plate in X-Z plane.....	18
Figure 4-13: LEU plate in Y-Z plane. ^{††}	18
Figure 4-14: HEU plate in X-Y plane, cutaway view.....	18
Figure 4-15: LEU plate in X-Y plane, cutaway view. ^{††}	18
Figure 4-16: Comparison of HEU and LEU standard fuel assemblies.....	19
Figure 4-17: Comparison of HEU and LEU shim safety fuel assemblies.....	20
Figure 4-18: Comparison of HEU and LEU regulating rod fuel assembly.....	20
Figure 4-19: Representation of HEU core load	21
Figure 4-20: Representation of LEU core load	21
Figure 4-21: HEU control rod calibration for SS-1	22
Figure 4-22: HEU control rod calibration for SS-2.....	23
Figure 4-23: HEU control rod calibration for RR.....	23
Figure 4-24: Calibration Curve for SS-1 Rod in LEU Core	24
Figure 4-25: Calibration Curve for SS-2 Rod in LEU Core	24
Figure 4-26: Calibration Curve for Regulating Rod in LEU Core	25
Figure 4-27: Figure showing water regions for perturbation models (LEU assemblies shown).....	28
Figure 4-28: Effect of Fuel Temperature, Water Temperature and Water Density Perturbations on HEU Core Reactivity.	31
Figure 4-29: Density of Sub-Cooled Water at 1.5 Atmospheres.....	32
Figure 4-30: PUR-1 Core Layout with LEU Fuel, SS-2 Inserted to Critical Position with SS-1 and RR Fully Removed.....	33
Figure 4-31: Effect of Fuel Temperature, Water Temperature and Water Density Perturbations on LEU Core Reactivity.	35
Figure 4-32: PUR-1 HEU Core Layout and Bundle Drawings	38
Figure 4-33: Heating Profile in Bundle 4-4 Plates.	41

Figure 4-34: Heating Profile in Plate 262 of Assembly 4-4 for Critical Positions 41

Figure 4-35: PUR-1 LEU Core Layout and Bundle Drawings..... 46

Figure 4-36: Axial Profiles in LEU Plates 1188, 1215 and 1348 for Critical Configurations.
..... 49

Figure 4-37: Radial Power Profiles in LEU Plates 1215 and 1348 for Critical
Configurations 50

Figure 4-38: Comparison of HEU and LEU Standard Fuel Elements..... 54

Figure 4-39: Comparison of HEU and LEU Standard Fuel Assembly 55

Figure 4-40: Comparison of HEU and LEU Control Fuel Elements 55

Figure 9-1: k-eff Values for Flooded Condition of Fuel Storage Facility. 64

1 GENERAL DESCRIPTION OF THE FACILITY

1.1 Introduction

This report contains the results of the design and safety analyses performed by the School of Nuclear Engineering at Purdue University, and the Reduced Enrichment for Research and Test Reactors (RERTR) Program at the Argonne National Laboratory (ANL) for the conversion of the Purdue University Reactor (PUR-1) from the use of Highly Enriched Uranium (HEU) fuel to Low Enriched Uranium (LEU) fuel. The objectives of this study were to: (1) maintain or improve upon the present reactor performance and safety margins, (2) maintain as closely as possible the technical specifications and operating procedures of the present HEU core, and (3) utilize a proven LEU fuel design.

The design and safety analyses in this report provide comparisons of reactor parameters and safety margins for the PUR-1 HEU and LEU cores. Only those parameters which could change as a result of replacing the HEU fuel in the core with LEU fuel are addressed. Documents that were reviewed by Purdue as bases for the design and safety evaluations were the PUR-1 Safety Analysis Report¹, the Technical Specifications for PUR-1², and the Safety Evaluation Report (NUREG-1283) for PUR-1³.

1.2 Summary and Conclusions of Principal Safety Considerations

The conclusions of this conversion proposal is that the new LEU core for PUR-1 meets or exceeds all of the requirements specified in the PUR-1 Technical Specifications [Ref. 2] and confirmed in the analyses of the SAR [Ref. 1].

1.3 Summary of Reactor Facility Changes

The LEU fuel assembly has the same overall design as the present HEU fuel assembly, except that it contains a maximum of 14 fueled plates with LEU U_3Si_2 -Al fuel, as opposed to a maximum of 10 fueled plates with HEU U-Al alloy fuel. A detailed evaluation of LEU U_3Si_2 -Al fuel can be found in NUREG-1313 published by the USNRC⁴.

1.4 Summary of Operating License, Technical Specifications, and Procedural Changes

There are no operational changes being proposed as a part of these analyses. Proposed changes in the Safety Limit (SL) and the Limiting Safety System Settings

(LSSS) Technical Specifications are described in Section 14 of this document. An additional change to the technical specification requiring inspection of fuel representative assemblies instead of representative individual fuel plates is proposed as well.

1.5 Comparison With Similar Facilities Already Converted

Similar pool-type, MTR reactors that are cooled by natural circulation have converted to the same LEU silicide plate-type fuels proposed for the PUR-1 conversion. They are the research reactors at the University of Missouri at Rolla and The Ohio State University, which are licensed to operate at power levels of 200 kW and 500 kW, respectively. Based on the performance of the fuel in these reactors, the LEU fuel performance in the 1kW PUR-1 should be equally good.

2 SITE CHARACTERISTICS

The conversion of PUR-1 from HEU to LEU fuel does not impact the site characteristics of the Purdue reactor facility as specified in Reference 1.

3 DESIGN OF STRUCTURES, SYSTEMS AND COMPONENTS

The conversion of PUR-1 from HEU to LEU fuel does not require any changes to the design of structure, systems, or components. More details about this topic can be found in Reference 1.

4 REACTOR DESCRIPTION

PUR-1 is a heterogeneous, pool-type non-power reactor. The core is cooled by natural convection of light water, moderated by light water, and reflected by water and graphite. The reactor is located near the bottom of a water-filled tank surrounded and supported by a concrete shielding structure as shown in Figure 4-1. An aluminum grid plate structure supports the reactor and control mechanisms at the bottom of the pool, with additional support of the control mechanisms provided by a fixture at the top of the pool. Three detectors used for monitoring reactor conditions are located in fixed positions next to the reactor core. And the startup detector is located in a tube affixed to a fuel element in the core, which allows the detector to be removed from the neutron flux when the reactor is at power.



Figure 4-1: PUR-1 Pool Layout

The reactor core is composed of sixteen fuel elements positioned in holes in the aluminum grid plate. The grid plate contains a rectangular matrix of holes to allow the changing of fuel element locations and the insertion of graphite reflector elements to displace reflector water. Each fuel element consists of several thin metal plates assembled into a unit about 7 cm by 7 cm with an active fuel length of approximately 60 cm. Fuel elements of this general configuration were first designed for and used in the Materials Testing Reactor (MTR) and thus are referred to as MTR-type fuel elements. Three of the fuel elements are fabricated without the four middle plates, providing space for the insertion and movement of the reactor control rods.

Reactivity of the reactor core is changed by the operator moving the control rods that are suspended from fail-safe electromagnets. The ionization chambers used for sensing neutron and gamma-ray fluxes are located near the core. The control console, from which the operator can observe the reactor pool and top structures, is located adjacent to the reactor, and consists of typical read-out and control instrumentation.

4.1 Reactor Facility

The HEU to LEU conversion of the PUR-1 facility requires only changes in the fuel assemblies. All of the following aspects of the facility remain unchanged:

- Control rods and drives
- Neutron reflector^{*}
- Neutron source[†]
- Reactor tank and biological shielding
- Core support structure
- Reactivity control system

No modifications of facility equipment that affect safety are required by the conversion.

The HEU and LEU cores contain plates that differ in composition of fuel meat, cladding material and thickness, enrichment and per plate fuel load. The current HEU core and expected LEU core also differ in the number of plates per assembly, total plates in the core, and number of fuel and dummy plates. Note that the expected LEU core configuration may differ when the actual fuel loading is performed.

Table 4-1 provides a comparison of the key design features of the HEU and LEU fuel. Table 4-2 presents a summary of the key reactor physics and safety parameters for the HEU and LEU cores.

^{*} The graphite neutron reflector elements will be removed from the current aluminum can assemblies and placed into new assembly cans of 6061 aluminum to match the new fuel. No design or functionality changes are being made to the assemblies, and no impact is expected on safety or performance by this change.

[†] The current neutron source will be removed from the current aluminum can assemblies and placed into a new 6061 aluminum can assembly. No design or functionality changes are being made to the assemblies, and no impact is expected on safety or performance by this change.

Table 4-1: Summary of Key Nominal Design Parameters of HEU (current) and LEU (Expected) Cores

DESIGN DATA	HEU	LEU
Fuel Type	MTR Plate	MTR Plate
Fuel "Meat" Composition	U-Al Alloy	U ₃ Si ₂ -Al
Fuel Enrichment U-235 (nominal)	93%	19.75%
Mass of U-235 per plate (g, nominal)	12.5	12.5
Fuel Meat Dimensions		
Width (mm)	62.7	59.6
Thickness (mm)	0.508	0.508
Height (mm)	600.1	600.1
Fuel Plate Dimensions		
Width (mm)	70.2	70.2
Thickness (mm)	1.52	1.27
Height (mm)	638.6	638.6
Cladding Composition	1100 Al	6061 Al
Cladding Thickness (mm)	0.508	0.381
Dummy Plate Composition	1100 Al	6061 Al
Dummy Plate Dimensions	Same as Fuel	Same as Fuel
Standard Fuel Assemblies		
Number of standard assemblies	13	13
Number of plates per standard assembly	10	14
Control Fuel Assemblies		
Number of control assemblies	3	3
Number of plates per control assembly	6	8
Total plates in core (fuel and dummy)	148	206
Fuel plates in core (current, expected)	124	190
Dummy plates in core (current, expected)	24	16
Plate spacing in standard assemblies (mm)	5.26	3.71
Plate spacing in control assemblies (mm)	5.26	5.00

Table 4-2: Summary of Key Reactor Physics and Safety Parameters for the HEU (current) and LEU (Expected) Cores

REACTOR PARAMETERS	HEU Measured	HEU Calculated	LEU Calculated
Fresh core excess reactivity (% $\Delta k/k$)	0.43	0.43 [†]	0.47 [§]
Shutdown margin (% $\Delta k/k$)	-2.07	-1.93 [†]	-1.53 [§]
Control rod worth (% $\Delta k/k$)			
Shim-safety 1	4.50	4.36	3.91
Shim-safety 2	2.52	2.35	2.00
Regulating Rod	0.28	0.27	0.29
Maximum reactivity insertion rate $\left(\frac{\% \Delta k}{k \cdot s}\right)$			
Shim-safety 1	1.12E-02	9.31E-03	1.84E-04
Shim-safety 2	7.45E-03	7.45E-03	1.07E-04
Regulating Rod	3.00E-02	2.25E-02	4.07E-05
Avg. coolant void coefficient $\left(\frac{\% \Delta k}{k \cdot \% \text{void}}\right)$		-9.88E-02	-1.68E-01
Coolant temperature coefficient $\left(\frac{\% \Delta k}{k \cdot ^\circ C}\right)$		-7.46E-03 ^{**}	-9.75E-03 ^{**}
Fuel temperature coefficient $\left(\frac{\% \Delta k}{k \cdot ^\circ C}\right)$		0	-9.91E-04
Effective delayed neutron fraction (%)		0.795	0.787
Neutron lifetime (μs)		76.7	81.3

4.2 Reactor Core

This section provides a description of the components and structures in the reactor core. Comparisons between the HEU and LEU cores are presented when changes due to conversion are required.

[†] Includes a bias of 0.32% $\Delta k/k$ for the HEU core, see Table 4-7: Comparison of calculated to measured critical rod positions for HEU core. The calculated excess reactivity is 0.75% $\Delta k/k$. The calculated shutdown margin is -1.61% $\Delta k/k$.

[§] Assumes the same bias as the HEU core. The calculated excess reactivity is 0.79% $\Delta k/k$. And the calculated shutdown margin is -1.31% $\Delta k/k$.

^{**} Calculated from 20-30°C.

The conversion of PUR-1 from HEU to LEU will utilize the same configuration of fuel assemblies, moderator, coolant, control elements, reflector, neutron source, and in-core experimental facilities. The pool tank layout will also remain the same, as will the grid support plate and core layout is shown in Figure 4-2.

The figure area is mostly blank, with a large, empty rectangular frame on the right side of the page, indicating that the visual content of Figure 4-2 is missing or not rendered in this document version.

Figure 4-2: PUR-1 Grid Plate

The PUR-1 core layout is a sixteen assembly (4x4 array), heterogeneous, light-water moderated, graphite reflected, water cooled reactor fueled with HEU plate-type U-Al fuel. Each of the thirteen standard fuel assemblies in the HEU core can hold up to 10 fuel plates, or a mixture of fuel and dummy plates.

The reactor is controlled by three control rods located in the core region of the reactor. There are two shim-safety rods made of solid borated 304 stainless steel, utilizing a magnet clutch between the blades and the lead screw operated drive mechanisms, and a regulating rod, which is a screw operated direct drive and made of hollow stainless steel. Each control blade is protected by an aluminum guide plate on each side within the control fuel assemblies.

Each ten-plate fuel element for the standard assemblies, and each set of two three-plate elements for the control assemblies, is contained in a 6061 aluminum

container. The standard graphite assemblies and the irradiation facility graphite assemblies are contained in similar 6061 aluminum containers. The startup neutron source is located outside the core in a similar 6061 aluminum container.

Heat removal is achieved by natural convection, with a general flow up through the nozzle at the bottom of the fuel assemblies. A drawing of the fuel assembly can is shown in Figure 4-3. This drawing is oriented 90 degrees counter-clockwise from the actual in-core orientation of the assembly can.



Figure 4-3: HEU fuel-assembly can with nozzle.

4.2.1 Fuel Elements

4.2.1.1 Fuel and Dummy Plates

The HEU and LEU fuel elements have similar overall designs, i.e. they are both composed of fuel plates consisting of a sandwich of fuel "meat" and aluminum cladding. The plates are then assembled into the elements consisting of a number of fuel and dummy plates, which are in turn inserted into the assembly cans. Details about the specifications of the PUR-1 LEU plates can be found in the Fuel Specifications.⁵

The major differences between the HEU and LEU cores are the fuel plates, specifically the enrichment, plate thickness, and the cladding material and thickness. The LEU fuel plates are thinner, with a thickness of 1.27mm (50 mils) versus the HEU plates with a thickness of 1.52 mm (60 mils). The cladding composition for the LEU plates is 6061 aluminum versus 1100 aluminum for the HEU. And the cladding thickness of the LEU cladding is 0.381mm (15 mils) versus 0.508 mm (20 mils) for the HEU. This information is shown in Table 4-3.

Table 4-3: Characteristics of the HEU and LEU Fuel Plates

	HEU ¹	LEU
Fuel Type	U-Al Alloy	U ₃ Si ₂ -Al
Fuel Plate Dimensions		
Width (mm)	70.2	70.2
Thickness (mm)	1.52	1.27
Height (mm)	638.6	638.6
Fuel Meat Dimensions		
Width (mm)	62.7	59.6 ²
Thickness (mm)	0.508	0.508
Height (mm)	600.1	600.1 ³
Cladding Type	1100 Al	6061 Al
Cladding:		
Along width (mm)	3.66 (min)	3.63 (min)
Along thickness (mm)	0.508	0.381

¹ Data taken from PUR-1 Drawing 117-0002, which corresponds to the LNP 1961 design.

² Drawing #635463 from INL shows values between 58.9mm and 62.7mm for the width of the fuel meat.

³ Drawing #635463 from INL shows values between 571.5mm and 609.6mm for the height of the fuel meat. This size was chosen to be the same as the HEU plates for the purposes of this analysis.

The HEU and LEU dummy plate dimensions are identical with their respective fuel plate dimensions. The dummy plates consist of 1100 aluminum for the HEU dummy plates, or 6061 aluminum for the LEU dummy plates.

4.2.1.2 Fuel Elements

Each standard HEU fuel element is composed of 10 plates, which may be either fuel or dummy plates (see Figure 4-4). The water gap between the HEU plates is nominally 5.26 mm. The bolt to bolt dimension is 71.25 mm. The LEU fuel elements are composed of 14 plates, which may be either fuel or dummy plates (see Figure 4-5). The water gap between the LEU plates is nominally 3.71 mm. The bolt to bolt dimension of the LEU elements is 69.72 mm.

Figure 4-4: HEU Fuel Element

Figure 4-5: LEU Fuel element

Each of the three control rods inserts into the core via a control assembly. The HEU control assemblies each contain a set of two control fuel elements with three plates each, which may contain either fuel or dummy plates. The water gap between the plates is uniform across the element at 0.526 cm.



Figure 4-6: HEU Control Fuel Element.

For the LEU core, the control fuel assemblies will contain a set of two fuel elements as well, with each element containing four plates, either fuel or dummy. The water gap between the plates is uniform across the element at 0.500 cm.



Figure 4-7: LEU Control Fuel Element.

4.2.1.3 Fuel Assemblies

Each of the standard fuel elements and the sets of two control elements are placed into a 6061 aluminum assembly can. The cans are to be replaced when the fuel is replaced, with newly manufactured cans of identical design, also made from 6061 aluminum. The gaps between the elements and assembly cans will be different between the HEU and LEU assemblies due to a design change in the hardware used to assemble the elements. The HEU fuel assembly is shown in Figure 4-8 and the LEU fuel assembly is shown in Figure 4-9.



Figure 4-8: HEU Standard Fuel Assembly



Figure 4-9: LEU Standard Fuel Assembly

4.2.2 Control Rods

No modifications of the control rods are required by the conversion of PUR-1 from HEU to LEU fuel. No changes to the design bases, mechanical design, absorber materials or core configuration will be made as part of the conversion process. The HEU and LEU models used in these analyses use the same rods.

4.2.3 Neutron Reflector

The graphite neutron reflector for PUR-1 will be reused, but will be placed in new 6061 Al cans to match the new cans for the fuel assemblies. Inspection of a sample graphite assembly in January 2006 showed that there has been no degradation of the graphite integrity, and replacement is not necessary. The conversion of the fuel from HEU to LEU is not expected to be affected by reusing the present graphite, nor is the conversion expected to be affected by replacement of the graphite assembly cans with new cans of the same alloy, 6061 aluminum.

4.2.4 Neutron Source Holder

No modifications of the startup neutron source configuration are required by the conversion of PUR-1 from HEU fuel to LEU fuel. A new container of the same design, function, construction, thermal and radiation properties, and construction material, 6061 aluminum, will replace the old one; however, no effects on performance are expected. The source drive mechanism is to remain the same.

4.2.5 In-Core Experimental Facilities

Irradiation facilities in the graphite reflector elements, identified as F4-F9 (see Figure 4-2 on page 7), are the only in-core experimental positions for PUR-1. These consist of 6061 aluminum tubes within the surrounding graphite and are filled with graphite for normal operation. The graphite in the tubes can be replaced with 6061 aluminum sample holders when the irradiation facilities are used.

The graphite reflector elements for PUR-1 are to be reused after the conversion to LEU fuel. New 6061 aluminum tubes are to be fabricated, however, which will be identical in design to the original facilities.

4.2.6 Reactor Materials

The conversion of PUR-1 to LEU fuel requires changing the fuel and cladding compositions. The LEU silicide fuel has been approved by USNRC for use in non-power reactors, and more detailed information can be found in Reference 4. Table 4-4 compares the material compositions of the HEU and LEU fuel plates.

Table 4-4: Composition of HEU and LEU Fuel

	HEU	LEU
Fuel "Meat"		
Composition	U-Al alloy	U ₃ Si ₂ -Al
Enrichment	93%	19.75%
Mass ²³⁵ U per fuel plate	1100 Al	12.5 g
Cladding composition	1100 Al	6061 Al

4.3 Reactor Tank and Biological Shield

No changes to the reactor tank and biological shield are required by the conversion from HEU to LEU fuel.

4.4 Core Support Structure

No changes to the core support structure are required by the conversion of PUR-1 from HEU to LEU fuel.

4.5 Dynamic Design

In order to best analyze the proposed LEU core, a detailed model of the HEU core was developed to determine operational and safety related parameters and compare them where possible to measured values and benchmarked data. Once a credible model for the HEU core was built, the model was modified to represent the LEU core model, making the geometry and material definition changes as necessary. These calculations utilized the MCNP5⁶ Monte Carlo code, with the ENDF-VI.5 continuous energy cross-section library. All calculations were done considering a fresh core loading for both the HEU and LEU cores, since PUR-1 has negligible depletion at a power of 1kW.

This section first provides a description of the HEU model, including the geometry and material definitions, and a comparison to measured data from PUR-1. The reference critical LEU model will then be described side by side with the HEU model to highlight the similarities and differences between the two cores. Where applicable, the calculated physics parameters for the LEU core are compared side by side with the HEU counterpart.

HEU Material Composition

The HEU reactor core was modeled as a fresh core only, since PUR-1 does not operate at a high enough power to consider depletion. Table 4-5 shows the elemental breakdown for all materials considered in the HEU model. Where materials characterizations were not available from the original vendors' communications, engineering assumptions were made and published guidelines for weight percentages were used.

Table 4-5: Material compositions used in HEU core model

Element	Weight %	Element	Weight %
HEU Fuel		1100 Al	
²³⁵ U]	Al	99.0000
²³⁸ U		Si	0.3346
Al		Fe	0.6654
		B	0.00001
SS-304M (borated)		6061 Al	
C	0.0670	Al	97.9000
Cr	19.4000	Si	0.6000
Mn	1.6100	Cr	0.2500
Fe	67.2490	Mg	1.0000
Ni	9.5400	Cu	0.2500
¹⁰ B	0.296	B	0.00001
P	0.0240		
S	0.0100	Graphite	
Si	0.6200	C	99.9999
		B	8.0E-06

HEU Model Geometry

A detailed MCNP5 model was developed for the HEU core, based on available engineering drawings and other available information. The regions included in the models include the reactor core, moderator, reflector, the reactor grid plate, neutron source, and the pool water surrounding the core.

HEU Model Verification

Once the HEU MCNP model was developed, several cases were run to establish the credibility of the model. An initial criticality case with all control rods at their upper limit gave a k_{eff} of 1.00753. Thus the reactivity bias is 0.32% $\Delta k/k$, as shown in Table 4-6.

Table 4-6: Calculated and Measured excess reactivity for fresh HEU core.

Measured Eigenvalue	Calculated HEU Eigenvalue	Bias (% $\Delta k/k$)
1.0043 ⁷	1.00753	0.32

Several cases were then run to compare the model to 5 measured critical rod positions. The first two cases were with SS-2 or SS-1 controlling, respectively, and the other rods at their upper limits. Case 3 was a banked rods condition. Case 4 had RR at its lower limit, SS-1 at its upper limit, and SS-2 controlling. Case 5 had RR near mid-core, SS-1 at the upper limit, and SS-2 controlling. Table 4-7 details the results.

Table 4-7: Comparison of calculated to measured critical rod positions for HEU core

Case	RR Position (cm)	SS-2 Position (cm)	SS-1 Position (cm)	Eigenvalue	Bias % $\Delta k/k$
1	64.12	43.60	64.12	1.00305	0.30
2	64.12	64.12	49.68	1.00285	0.29
3	51.93	51.92	53.19	1.00327	0.33
4	1.89	54.40	64.12	1.00340	0.34
5	31.44	48.47	64.12	1.00327	0.33

The data from these cases reflect a consistent model bias, with an average bias of 0.32% $\Delta k/k$. More cases were then run for additional comparisons to measured reactor parameters. Control rod worths were calculated for each control rod and compared to measured values, which are re-measured each year as part of the annual inspection. This data, shown in Table 4-8, also shows good agreement between measured and calculated values.

Table 4-8: Comparison of measured and calculated control rod worths for HEU core

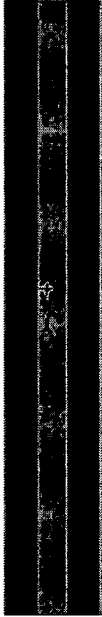
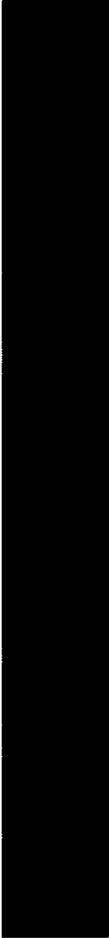
	Measured Value ($\Delta k/k$)	Calculated Value ($\Delta k/k$)	Error %
Shim Safety 1	0.0450	0.0436	-3.11%
Shim Safety 2	0.0252	0.0235	-6.74%
Regulating Rod	0.0028	0.0027	-3.57%

Based upon the good agreement of the HEU model with measured core parameters, an LEU model was then built that utilized a similar geometry to the HEU core. A more detailed explanation of the differences between the HEU and LEU models is in a later section.

The LEU Model

For the LEU model, the HEU plates and dummies are replaced with LEU plates and dummies. Two of the three outer dimensions of the LEU plates are similar to their HEU counterparts, namely the length and width. Nominal values for the HEU and LEU plates are shown in Table 4-3. The material composition for the plates was changed as well, with the U_3Si_2 -Al replacing the U-Al alloy, and 6061 aluminum replacing the 1100 aluminum cladding. Representations of the HEU and LEU plates are shown in Table 4-9. Another difference in the LEU model was the addition of 20 parts per million of a boron-equivalent to the 6061 cladding material to account for impurities in the alloy. The 1100 aluminum cladding of the HEU fuel was assumed to have a 10 ppm boron content, as were the 6061 aluminum assembly cans.

Table 4-9: Representation of HEU and LEU fuel plates.

 <p>Figure 4-10: HEU plate in X-Z plane</p>	 <p>Figure 4-11: HEU plate in Y-Z plane^{††}</p>	 <p>Figure 4-12: LEU plate in X-Z plane</p>	 <p>Figure 4-13: LEU plate in Y-Z plane.^{††}</p>
 <p>Figure 4-14: HEU plate in X-Y plane, cutaway view.^{‡‡}</p>			
 <p>Figure 4-15: LEU plate in X-Y plane, cutaway view.^{‡‡}</p>			

^{††} Note: This represents a cutaway view, near the middle of the plate, not the same scale as X-Z view, as it was enlarged to show more detail. It also does not show the full length of the plate.

^{‡‡} Note: This represents a cutaway view near the middle of the plate, and is not the same scale as the X-Z view, it was enlarged to show more detail. Green surrounding the plate is water.

The representations of the complete standard and shim safety control fuel assemblies for the HEU and LEU cores are shown in Figure 4-16 and Figure 4-17 respectively. The regulating rod assemblies for the HEU and LEU core are shown in Figure 4-18. There are two dummy plates in both the HEU and LEU standard assemblies, which are the plates without the center fuel material in the figures. The differences that should be noted in the standard assemblies are the plate thicknesses and spacing. The assembly cans are identical in size and composition.

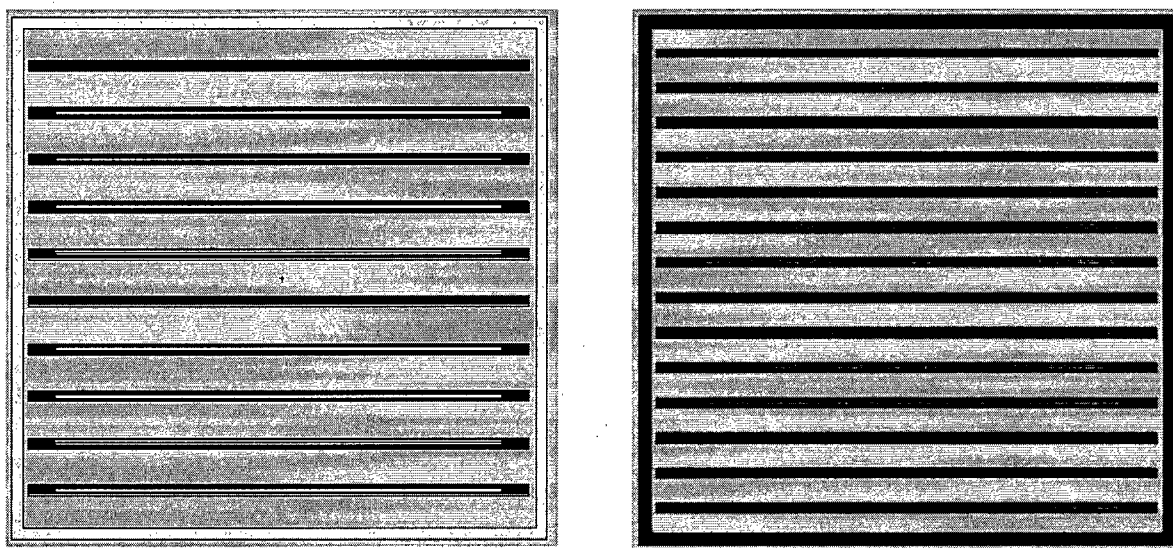


Figure 4-16: Comparison of HEU and LEU standard fuel assemblies.

The shim safety control assemblies contain no dummy plates, but do contain a guard plate made of 6061 aluminum between the fuel elements and the control rods to prevent any mechanical damage to the fuel from insertion of the control rods. The control rods themselves, made of borated stainless steel, are oblong shaped plates inserted down the center of the assemblies. They are identical in both models.

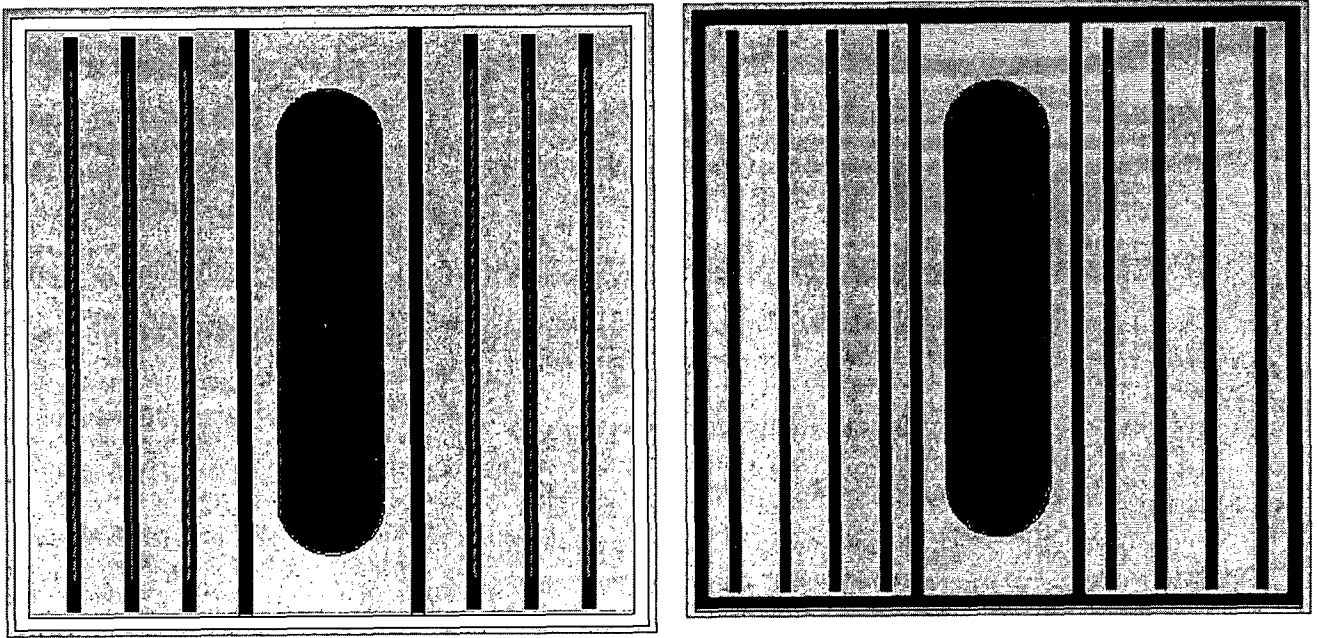


Figure 4-17: Comparison of HEU and LEU shim safety fuel assemblies.

The regulating rod differs from the shim safety rods in that it is hollow, non-borated stainless steel filled with water. The rest of the assembly is identical to the shim safety rod assemblies for both the HEU and LEU cores. The regulating rod itself is identical between the two models.

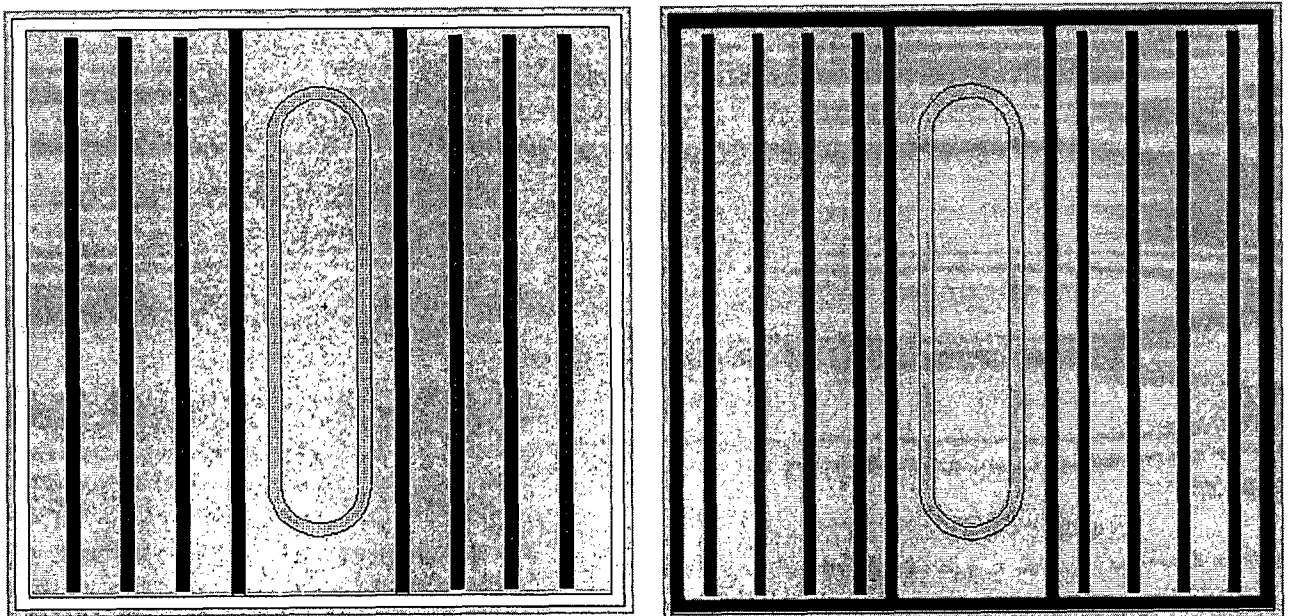


Figure 4-18: Comparison of HEU and LEU regulating rod fuel assembly

Figure 4-19 and Figure 4-20 are representations of the HEU and LEU cores, respectively. The layout and overall core dimensions are the same between the two models. The only differences are within the fuel assemblies.



Figure 4-19: Representation of HEU core load

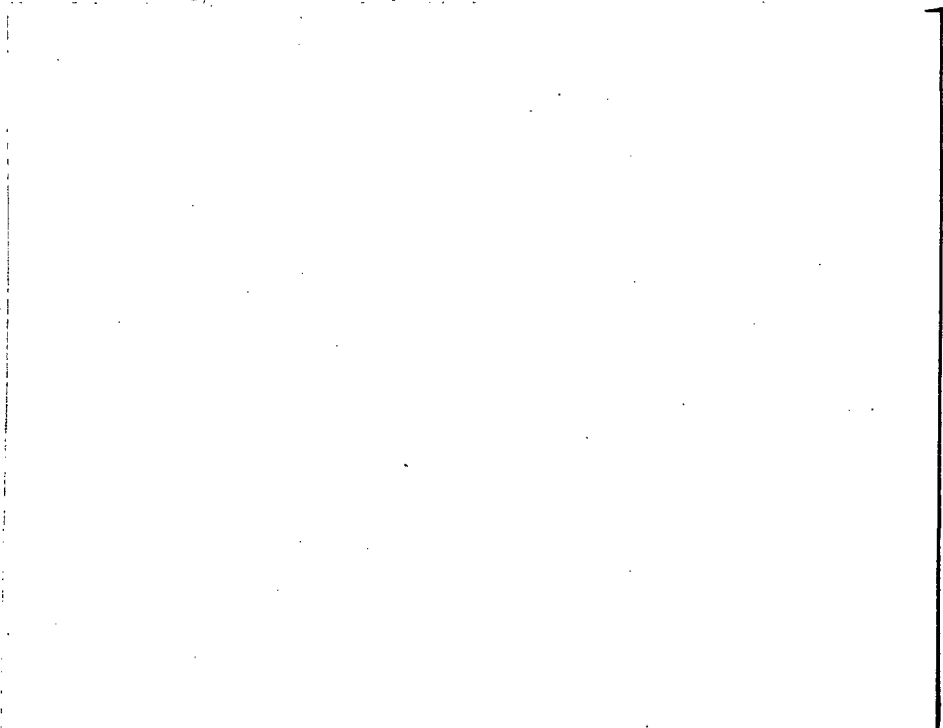


Figure 4-20: Representation of LEU core load

Using the LEU model developed above, the pertinent core parameters and conditions were evaluated for the analyses.

4.5.1 Control Rod Worths and Excess Reactivity

Excess reactivity of the LEU core in PUR-1 was determined to be 0.00468 (0.47%) $\Delta k/k$ in a 190 fuel plate core (16 dummies), including a reactivity bias of 0.32% $\Delta k/k$. This value is within the Technical Specification limit of 0.6% for excess reactivity.

Control rod worths were calculated for the HEU core and compared with measured data. The calculated and measured control rod worth values are shown in Table 4-10. Figure 4-21, Figure 4-22, and Figure 4-23 show the calibration curve data comparison for Shim-safety 1, Shim-safety 2 and the Regulating Rod respectively

Table 4-10: Comparison of HEU and LEU calculated control rod worths.

	HEU Calculated ($\Delta k/k$)	LEU Calculated ($\Delta k/k$)
Shim Safety 1	0.0436	0.0391
Shim Safety 2	0.0235	0.0200
Regulating Rod	0.0027	0.0029

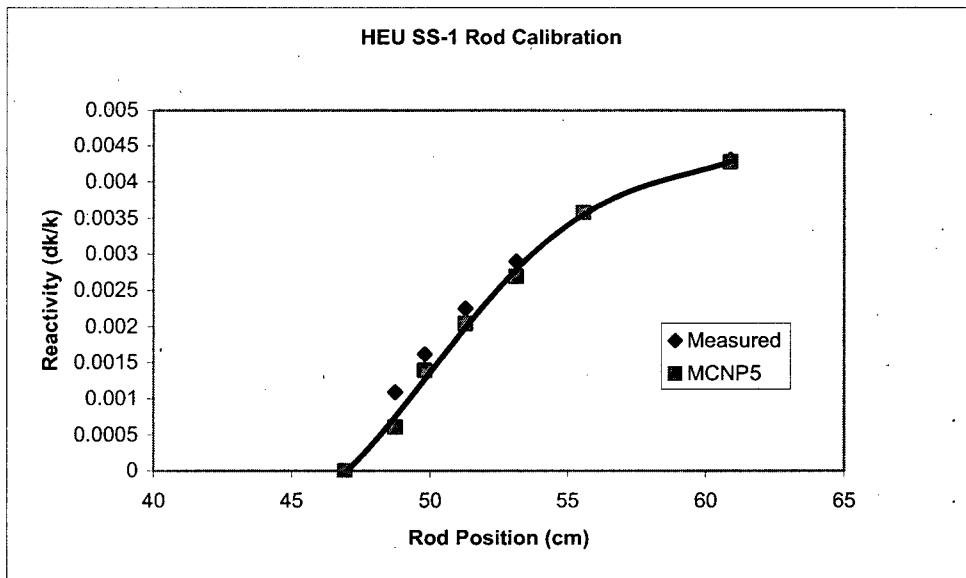


Figure 4-21: HEU control rod calibration for SS-1

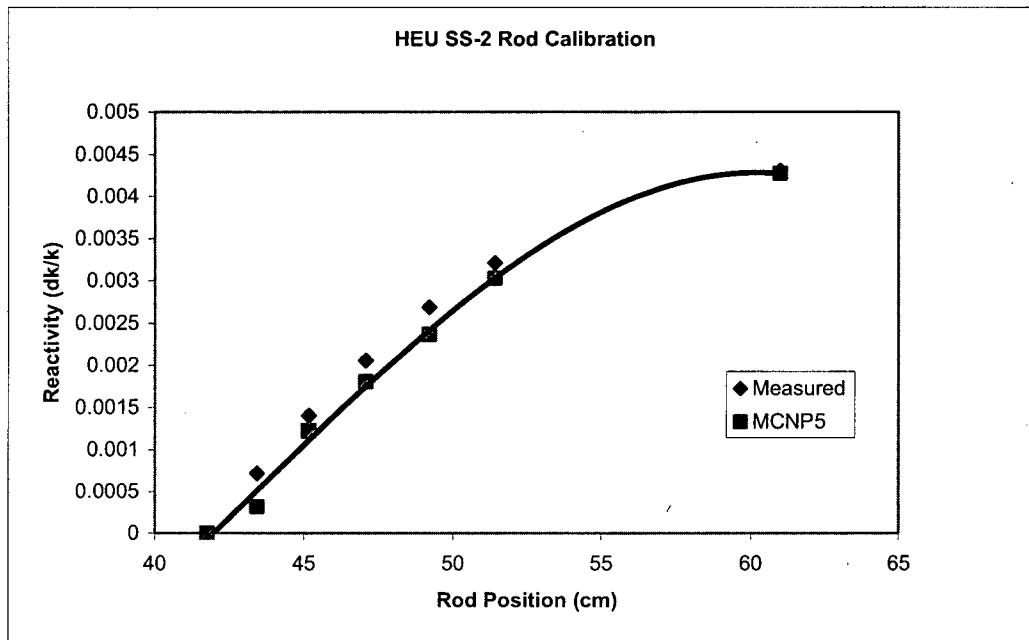


Figure 4-22: HEU control rod calibration for SS-2

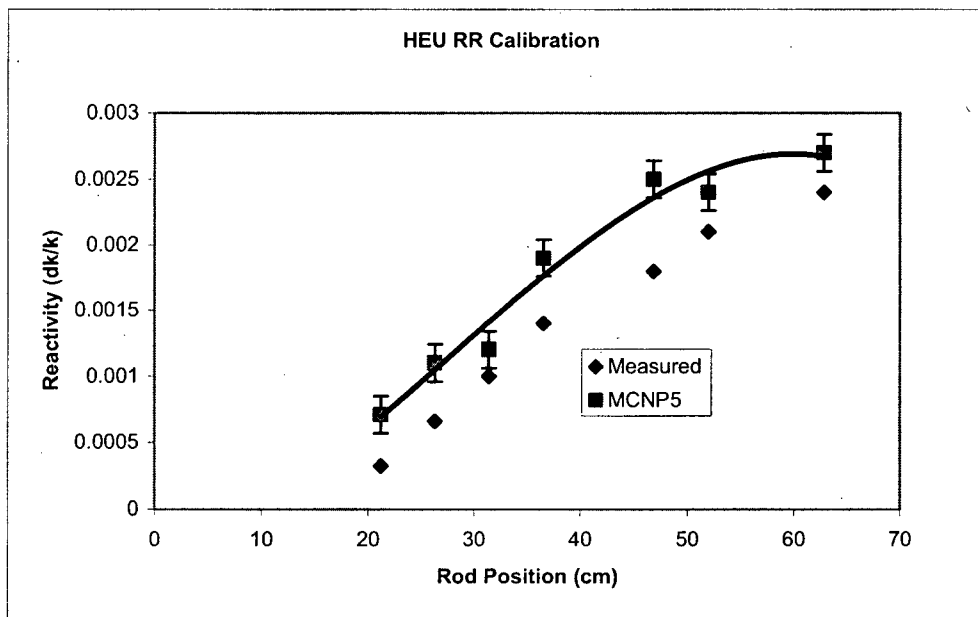


Figure 4-23: HEU control rod calibration for RR

The calibration curves were then done for the LEU core. Figure 4-24, Figure 4-25, and Figure 4-26 show the calculated control rod worth curves for each of the control rods.

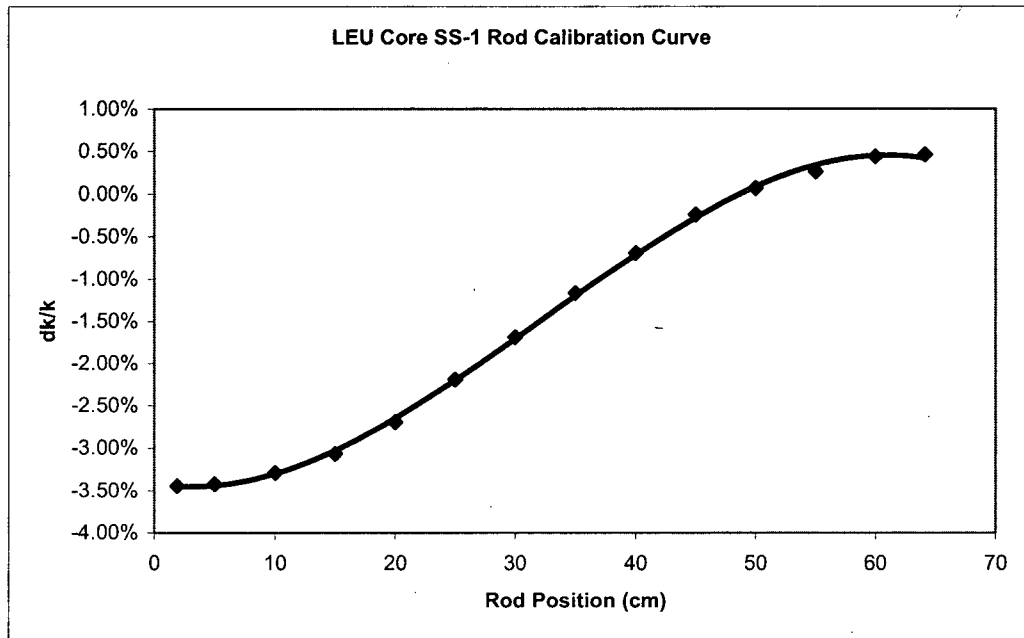


Figure 4-24: Calibration Curve for SS-1 Rod in LEU Core

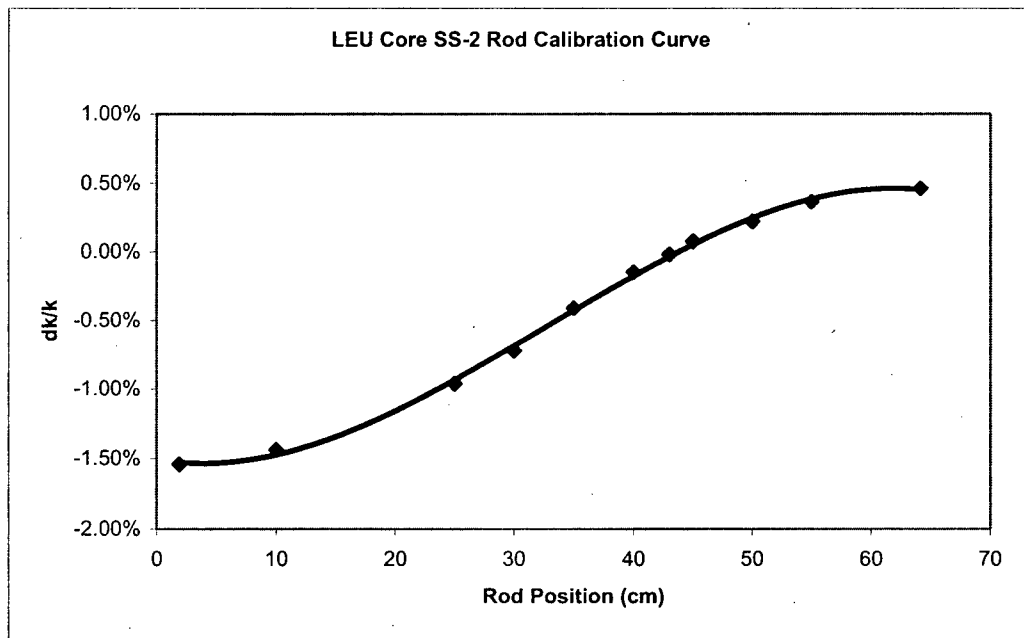


Figure 4-25: Calibration Curve for SS-2 Rod in LEU Core

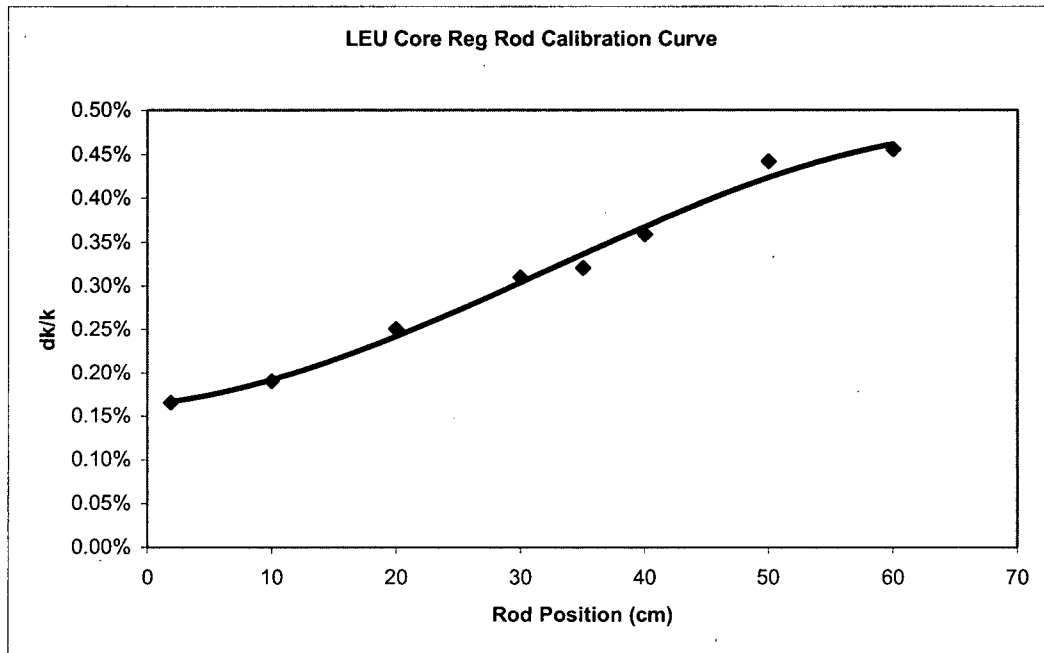


Figure 4-26: Calibration Curve for Regulating Rod in LEU Core

Using the rod worth curves in preceding figures, the maximum reactivity insertion rates were determined by finding the maximum slope, or rate of change, of the curve. The comparison of calculated and measured maximum reactivity insertion rates for the LEU and HEU cores are shown in Table 4-11.

Table 4-11: Comparison of maximum reactivity insertion rates for HEU and LEU cores

	Maximum Reactivity Insertion Rates for Control Rods $\left(\frac{\Delta k}{k \cdot s}\right)$		
	HEU Measured	HEU Calculated	LEU Calculated
Shim-safety 1	1.12E-04	9.31E-05	1.84E-04
Shim-safety 2	7.45E-05	7.45E-05	1.07E-04
Regulating Rod	3.00E-04	2.25E-05	4.07E-05

4.5.2 Shutdown Margin

The shutdown margin was calculated for the HEU and LEU cores, and compared to the measured HEU core values in Table 4-12. The calculated shutdown margin for the LEU core meets the technical specification (TS 3.1.a).

Table 4-12: Comparison of shutdown margins for HEU and LEU cores

	HEU Measured	HEU Calculated	LEU Calculated
SS-2 Worth	-0.02366	-0.02350	-0.0200
k_{excess}	0.00431	0.00423	0.00468
Shutdown Margin ($\Delta k/k$)	-1.94%	-1.93%	-1.53%

4.5.3 Other Core Physics Parameters

Reactivity coefficients and reactor kinetics parameters were calculated for both the HEU and LEU cores. These values are used to estimate the core reactivity response to changes in properties of the fuel temperature, coolant/moderator temperature, or coolant/moderator density. They are therefore essential for analyses of reactivity-induced transients. These calculations were performed with the MCNP5 code using the same core model as for the core design and power distribution analyses.

The reactor kinetics parameters evaluated for PUR-1 were the effective delayed neutron fraction, β_{eff} , and the prompt neutron lifetime, ℓ . The effective delayed neutron fraction is calculated using two eigenvalue calculations from MCNP5. Normal calculations of k_{eff} include both prompt and delayed neutrons. A additional calculation of k_{eff} is performed with delayed neutrons turned off in MCNP, yielding a k_{eff} that depends only on prompt neutrons, which is denoted by $k_{\text{eff}}^{\text{prompt}}$. The effective delayed neutron fraction is then defined as

$$\beta_{\text{eff}} = 1 - \frac{k_{\text{eff}}^{\text{prompt}}}{k_{\text{eff}}}$$

The prompt neutron lifetime is calculated using the “1/v insertion method,” where a uniform concentration of a 1/v absorber such as ^{10}B is included at a very dilute concentration everywhere in the core and the reflector. The prompt neutron lifetime, ℓ , is calculated by

$$l = \lim_{N \rightarrow 0} \left[\frac{\frac{k_1 - k_0}{k_1}}{N_1 \sigma_a v} \right],$$

where k_1 is the k_{eff} of the system with a uniform concentration, N_1 , of a $1/v$ absorber, and σ_a is the infinitely-dilute absorption cross section of the absorber for neutrons at speed v . For this effort, the ^{10}B absorption cross section is assumed to be $\sigma_a=3837$ barns for a neutron speed of $v=2200$ m/s.

Reactivity coefficients provide an estimate of the reactivity response to changes in state properties, given as:

$$\Delta\rho = \alpha_x \cdot \Delta x$$

where α_x is the reactivity coefficient due to a unit change in property x , and Δx is the value change for property x . The reactivity coefficients are calculated assuming that simultaneous changes in multiple state properties are separable. These are calculated from core eigenvalue calculations with independent perturbations to state properties, as shown here:

$$\alpha_x = \frac{\Delta\rho}{\Delta x} = \frac{k_1 - k_0}{k_1 k_0} \cdot \frac{1}{(x_1 - x_0)}$$

PUR-1 operates at a maximum power of 1 kW and is cooled by natural convection. The nominal conditions for the core used in the reactor design model assumed fresh fuel (i.e., no fission products given the low burnup of the PUR-1), isothermal conditions of 20°C, and impurities in the fuel, clad, and graphite based on the best-available data.

The reactivity coefficients are calculated assuming separability of the reactivity feedback effects due to changes in fuel temperature, water temperature, and water density. After establishing a nominal state based on the conditions given above and a critical rod configuration determined in the reactor design analysis, cases with perturbations to the temperatures or water density were evaluated.

The fuel temperature changes are assumed to occur uniformly throughout the reactor (i.e. the same temperature perturbation in all fuel plates), while the water temperatures or densities were perturbed in different zones of the reactor depending on

the proximity to the fuel plates. In the time immediately after the initiation of a reactivity induced transient, the water inside the fuel assembly can (shown in light blue in Figure 4-27) would heat up and have a feedback effect on the transient. However, the water between the cans and also in the space between the control rod and guard plates (shown in orange in Figure 4-27) would take some time to be heated as a result of a power increase from the transient due to the slow water circulation time with natural convection cooling. It would take even longer for the water in the reactor tank to be heated. Consequently, cases were evaluated with the water temperature or density perturbed:

- within the fuel assembly (light blue regions in Figure 4-27)
- within the fuel assembly and the water between the assemblies (orange regions in Figure 4-27), and
- within the fuel assembly, the water between the assemblies, and the pool or reflector water (all of the water in the MCNP5 model).

For the evaluation of the reactivity induced transients, only the reactivity coefficients calculated by perturbing the fuel assembly water will be used.

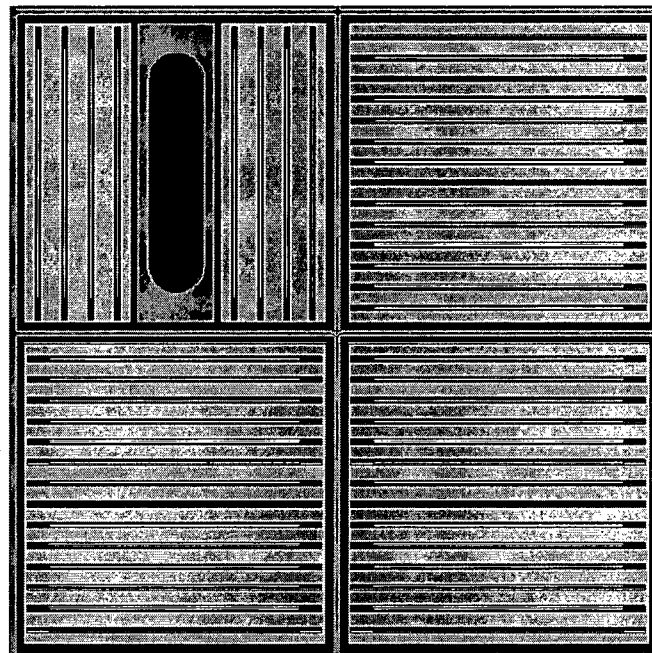


Figure 4-27: Figure showing water regions for perturbation models (LEU assemblies shown)

A summary of the values determined in the analyses of the HEU and LEU reactor physics parameters and reactivity coefficients is presented in Table 4-13. Explanations of the analyses for the HEU and LEU cores are provided in Sections 4.5.3.1 and 4.5.3.2, respectively.

Table 4-13: Comparison of other core physics parameters for HEU and LEU cores

	HEU (calculated)	LEU (calculated)
$\alpha_{\text{fuel}} \left(\frac{\% \Delta k}{k \cdot ^\circ \text{C}} \right)$	0	-9.91E-04
$\alpha_{\text{moderator}} \left(\frac{\% \Delta k}{k \cdot ^\circ \text{C}} \right)$	-7.46E-03	-9.75E-03
$\alpha_{\text{void}} \left(\frac{\% \Delta k}{k \cdot \% \text{void}} \right)$	-9.88E-02	-1.68E-01
β_{eff}	0.795%	0.787%
ℓ (μs)	76.7	81.3

4.5.3.1 HEU Core Results

For the HEU core, five different critical rod configurations based on experiments with the existing core were evaluated to benchmark the MCNP5 model (see Table 4-7). Heating tallies with neutron and photon transport were used to determine the power distribution in the reactor. It was found that the so-called “50-50-50” rod configuration, in which the two shim and one regulating rods were banked with the rod tips at about 50 cm from the bottom of the fuel element, gave the highest peak-to-average power density. The resulting power distribution was used in the thermal-hydraulics analysis of the HEU core. The HEU core model with this same rod configuration was used when calculating the HEU reactivity coefficients and kinetics parameters.

Figure 4-28 shows the effects of the fuel and water temperature, and water density perturbations on the HEU core reactivity. Because of the low U-238 content in the HEU fuel, increasing the fuel temperature causes a slight increase in the HEU core reactivity because of broadening of the U-235 fission resonances. However, the reactivity increase from a fuel temperature perturbation is negligible, especially when

compared with the negative feedback effects from water temperature and density effects.

Increasing the water temperature has a significant negative reactivity feedback. The mean energy of neutrons in the thermal energy range increases, hardening the neutron spectrum and decreasing the U-235 absorption cross section. The reactivity decrease for a given temperature perturbation is largest when only the water inside the fuel bundle can (labeled "FA Water" in Figure 4-28) is perturbed. Increasing the temperature of the water between the cans ("IA") or in the reactor tank outside the core ("REF") reduces the neutron capture rate in the water because of a reduction in the hydrogen absorption cross section. Thus, the reactivity change becomes smaller in magnitude, and is even slightly positive for small changes in the tank water temperature.

The reactivity feedback due to water density perturbations which would result from temperature increases was also evaluated. The water density corresponding to a given temperature was adjusted as shown in Figure 4-29, which shows the density of sub-cooled water as a function of temperature for water at 1.5 atmospheres. This corresponds to the coolant pressure of the PUR-1, which is under about 15 feet of water from the top of the reactor tank to the inlet to the fuel assembly channels. Decreasing the water density hardens the neutron spectrum, and also increases the neutron leakage. For a change in water conditions due to a given temperature change, the reactivity feedback due to the water density is smaller in magnitude than that due to temperature.

Table 4-14 summarizes the reactivity feedback coefficients for water temperature and density perturbations for the HEU core. The fuel temperature coefficient can be treated as negligible, so it is not included in Table 4-14. Coefficients were calculated based on a linear fit between the calculated data points. The water temperature coefficient becomes more negative as the water temperature is increased. For the sake of conservatism in the accident analyses, it is recommended to use the temperature coefficient with the smallest magnitude, which occurs over the temperature range from 20°C to 30°C. It is also recommended to use the temperature coefficient that results from heating of the fuel assembly water only, i.e. the water between the fuel plates, neglecting any heating of the water between fuel bundles or in the reactor tank. The

smallest magnitude for the water density (or void) coefficient occurs over the effective temperature range of 40°C to 60°C.

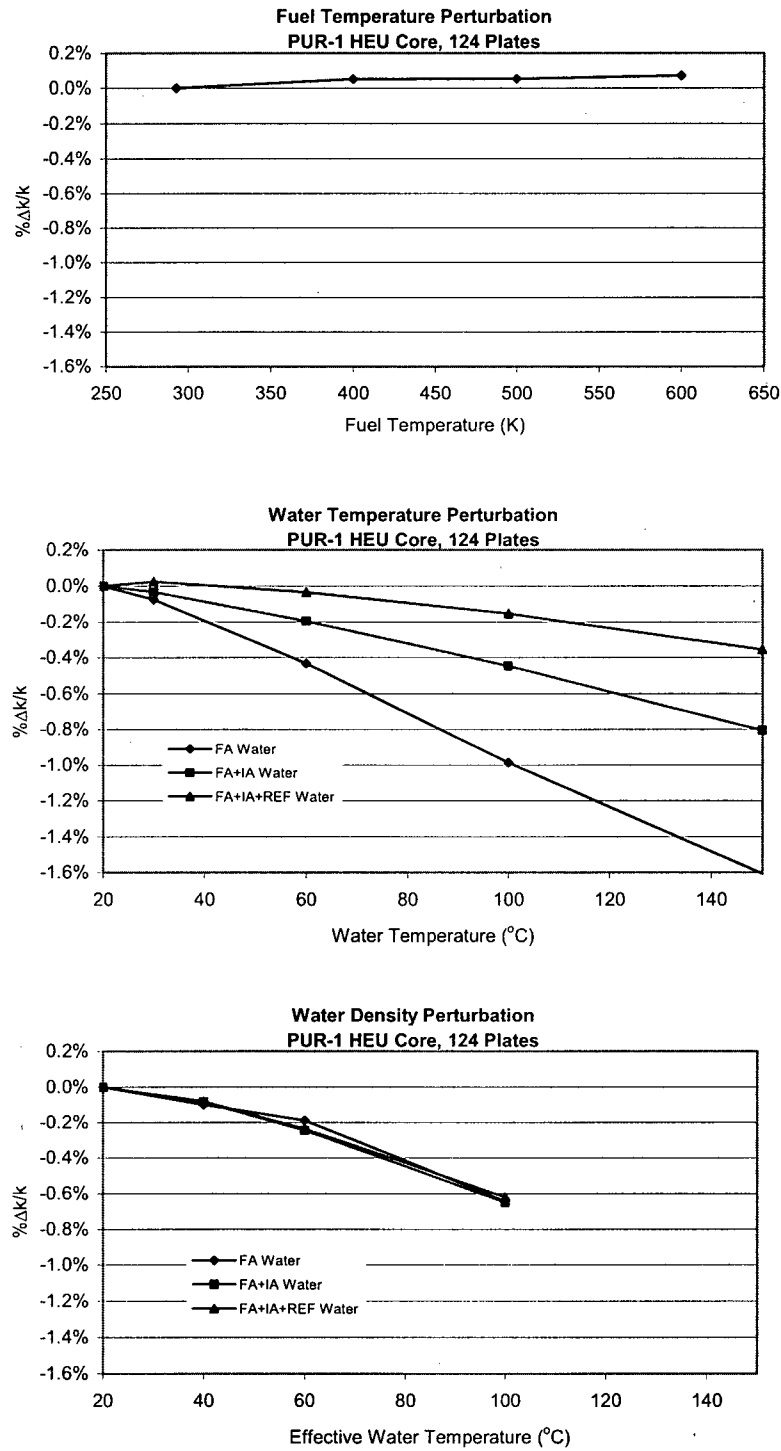


Figure 4-28: Effect of Fuel Temperature, Water Temperature and Water Density Perturbations on HEU Core Reactivity.

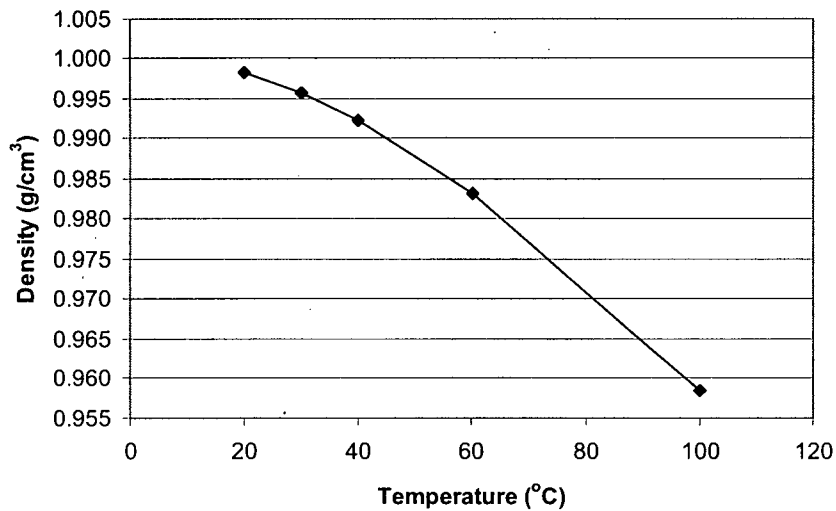


Figure 4-29: Density of Sub-Cooled Water at 1.5 Atmospheres.

Table 4-14: Water and Fuel Non-Isothermal Temperature Coefficients for PUR-1 HEU Core (Void coefficients are Shown in Units of $\Delta\rho/^\circ\text{C}$ and $\Delta\rho/\%\text{void}$).

Fuel Assembly Water Only						
$\alpha_{\text{water}} =$	-7.460E-05	$\Delta\rho/^\circ\text{C}$	(20 to 30 °C)			
$\alpha_{\text{water}} =$	-1.192E-04	$\Delta\rho/^\circ\text{C}$	(30 to 60 °C)			
$\alpha_{\text{water}} =$	-1.384E-04	$\Delta\rho/^\circ\text{C}$	(60 to 100 °C)			
$\alpha_{\text{void}} =$	-4.968E-05	$\Delta\rho/^\circ\text{C}$	(20 to 40 °C)	-1.650E-03	$\Delta\rho/\%\text{ void}$	(0 to 0.60% void)
$\alpha_{\text{void}} =$	-4.480E-05	$\Delta\rho/^\circ\text{C}$	(40 to 60 °C)	-9.878E-04	$\Delta\rho/\%\text{ void}$	(0.60% to 1.50% void)
$\alpha_{\text{void}} =$	-2.272E-04	$\Delta\rho/^\circ\text{C}$	(60 to 100 °C)	-1.797E-03	$\Delta\rho/\%\text{ void}$	(1.50% to 3.99% void)
Fuel and Inter-assembly water						
$\alpha_{\text{water}} =$	-3.182E-05	$\Delta\rho/^\circ\text{C}$	(20 to 30 °C)			
$\alpha_{\text{water}} =$	-5.446E-05	$\Delta\rho/^\circ\text{C}$	(30 to 60 °C)			
$\alpha_{\text{water}} =$	-6.302E-05	$\Delta\rho/^\circ\text{C}$	(60 to 100 °C)			
$\alpha_{\text{void}} =$	-4.222E-05	$\Delta\rho/^\circ\text{C}$	(20 to 40 °C)	-1.403E-03	$\Delta\rho/\%\text{ void}$	(0 to 0.60% void)
$\alpha_{\text{void}} =$	-8.017E-05	$\Delta\rho/^\circ\text{C}$	(40 to 60 °C)	-1.768E-03	$\Delta\rho/\%\text{ void}$	(0.60% to 1.50% void)
$\alpha_{\text{void}} =$	-2.018E-04	$\Delta\rho/^\circ\text{C}$	(60 to 100 °C)	-1.596E-03	$\Delta\rho/\%\text{ void}$	(1.50% to 3.99% void)
All Water						
$\alpha_{\text{water}} =$	2.385E-05	$\Delta\rho/^\circ\text{C}$	(20 to 30 °C)			
$\alpha_{\text{water}} =$	-1.922E-05	$\Delta\rho/^\circ\text{C}$	(30 to 60 °C)			
$\alpha_{\text{water}} =$	-2.987E-05	$\Delta\rho/^\circ\text{C}$	(60 to 100 °C)			
$\alpha_{\text{void}} =$	-3.974E-05	$\Delta\rho/^\circ\text{C}$	(20 to 40 °C)	-1.320E-03	$\Delta\rho/\%\text{ void}$	(0 to 0.60% void)
$\alpha_{\text{void}} =$	-7.867E-05	$\Delta\rho/^\circ\text{C}$	(40 to 60 °C)	-1.735E-03	$\Delta\rho/\%\text{ void}$	(0.60% to 1.50% void)
$\alpha_{\text{void}} =$	-1.907E-04	$\Delta\rho/^\circ\text{C}$	(60 to 100 °C)	-1.509E-03	$\Delta\rho/\%\text{ void}$	(1.50% to 3.99% void)

The calculation the Prompt Neutron Lifetime and Delayed Neutron Fraction were calculated for the HEU core using the methods described in Section 4.5.3. The prompt neutron lifetime for the HEU core was calculated to be 76.7 μ s. The effective delayed neutron fraction for the HEU core was calculated as $\beta_{\text{eff}}=0.795\%$.

4.5.3.2 LEU Core Results

For the LEU core, two different critical rod configurations were determined from the reactor design analysis. These were derived assuming the reactivity bias for the LEU core model as determined for the HEU core. A rod configuration with the SS2 rod inserted at 43 cm, and the SS1 and regulating rods fully withdrawn, was found to result in the largest peak-to-average power density. The location of the SS2 rod is indicated by the oblong steel rod shown in Figure 4-30. This critical rod configuration was modeled in the LEU core reactivity coefficients and kinetics parameters calculations.



Figure 4-30: PUR-1 Core Layout with LEU Fuel, SS-2 Inserted to Critical Position with SS-1 and RR Fully Removed.

Figure 4-31 shows the effects of the fuel and water temperature, and water density perturbations on the LEU core reactivity. The LEU core has a negative fuel temperature coefficient because of the Doppler effect on the U-238 capture resonances in the LEU fuel. The fuel temperature coefficient is smaller than that from water

temperature or density effects, but it is a non-negligible parameter for the LEU accident analyses.

The behavior of the LEU core reactivity due to water temperature and density perturbations is quite similar to that for the HEU core. The LEU core does have a harder neutron spectrum under nominal conditions, so the spectrum hardening due to the water temperature increase should have a smaller feedback effect on the core reactivity. On the other hand, coolant voiding in the LEU core results in greater neutron leakage because of the harder spectrum, so the negative reactivity feedback effect due to the reduced water density is greater for the LEU core.

Table 4-15 summarizes the reactivity feedback coefficients for water temperature and density, and fuel temperature perturbations for the LEU core. As for the HEU core, the water temperature coefficient becomes more negative as the water temperature is increased. The temperature coefficient calculated over the range from 20°C to 30°C for the “fuel assembly” water should be used for the accident analyses. It should be noted that the water temperature coefficient over this range is actually larger than the HEU core. For the water density feedbacks, the coefficient calculated over the range from 40°C to 60°C is the most conservative value for the accident analyses.

The effective delayed neutron fraction and prompt neutron lifetime were calculated in the same manner as for the HEU core. The calculated values are $\beta_{\text{eff}}=0.787\%$ and $\ell=81.3 \mu\text{s}$. The delayed neutron fraction is smaller and the prompt neutron lifetime is longer for the LEU core because of the harder spectrum.

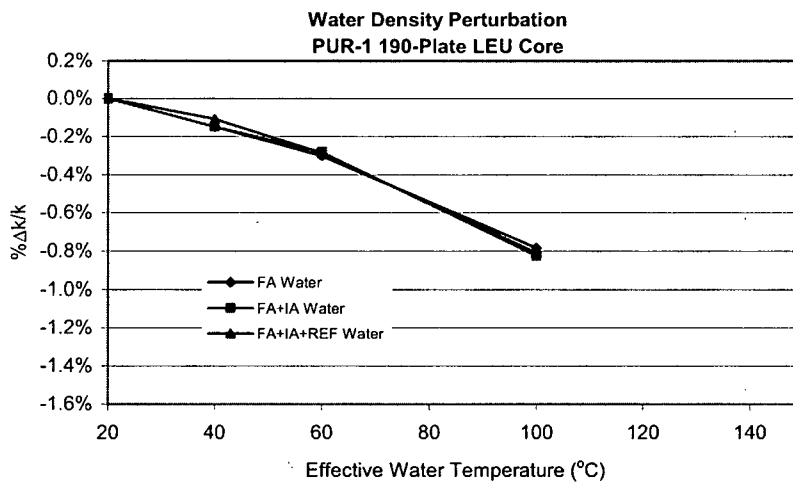
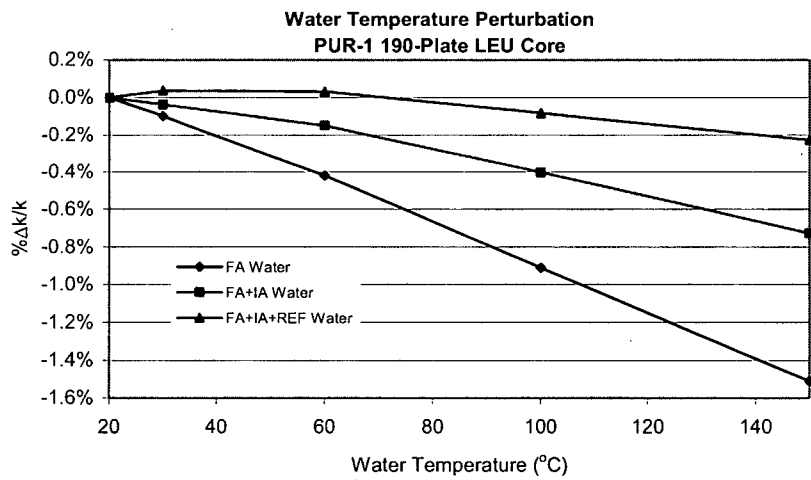
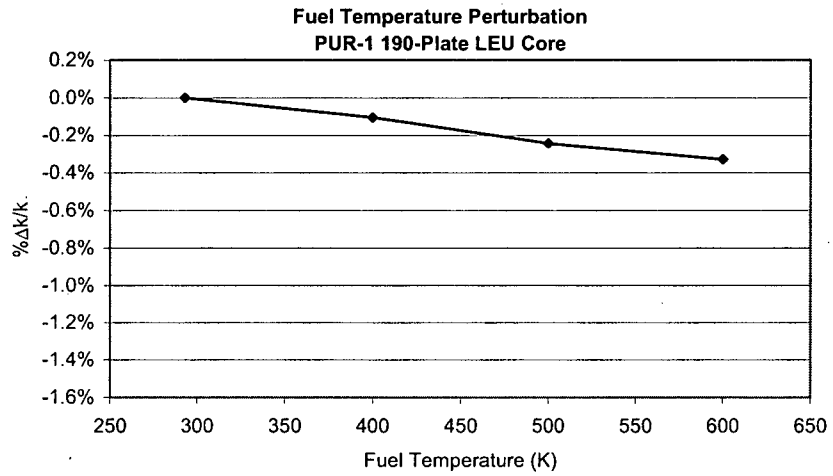


Figure 4-31: Effect of Fuel Temperature, Water Temperature and Water Density Perturbations on LEU Core Reactivity.

Table 4-15: Water and Fuel Non-Isothermal Temperature Coefficients for PUR-1 LEU Core (Void coefficients are Shown in Units of $\Delta\rho/^\circ\text{C}$ and $\Delta\rho/\%\text{void}$).

Fuel Assembly Water Only						
$\alpha_{\text{water}} =$	-9.747E-05	$\Delta\rho/^\circ\text{C}$	(20 to 30 °C)			
$\alpha_{\text{water}} =$	-1.075E-04	$\Delta\rho/^\circ\text{C}$	(30 to 60 °C)			
$\alpha_{\text{water}} =$	-1.229E-04	$\Delta\rho/^\circ\text{C}$	(60 to 100 °C)			
$\alpha_{\text{void}} =$	-7.455E-05	$\Delta\rho/^\circ\text{C}$	(20 to 40 °C)	-2.476E-03	$\Delta\rho/\%\text{ void}$	(0 to 0.60% void)
$\alpha_{\text{void}} =$	-7.627E-05	$\Delta\rho/^\circ\text{C}$	(40 to 60 °C)	-1.682E-03	$\Delta\rho/\%\text{ void}$	(0.60% to 1.50% void)
$\alpha_{\text{void}} =$	-1.209E-04	$\Delta\rho/^\circ\text{C}$	(60 to 100 °C)	-1.913E-03	$\Delta\rho/\%\text{ void}$	(1.50% to 3.99% void)
Fuel and Inter-assembly Water						
$\alpha_{\text{water}} =$	-3.777E-05	$\Delta\rho/^\circ\text{C}$	(20 to 30 °C)			
$\alpha_{\text{water}} =$	-3.717E-05	$\Delta\rho/^\circ\text{C}$	(30 to 60 °C)			
$\alpha_{\text{water}} =$	-6.345E-05	$\Delta\rho/^\circ\text{C}$	(60 to 100 °C)			
$\alpha_{\text{void}} =$	-7.455E-05	$\Delta\rho/^\circ\text{C}$	(20 to 40 °C)	-2.476E-03	$\Delta\rho/\%\text{ void}$	(0 to 0.60% void)
$\alpha_{\text{void}} =$	-6.628E-05	$\Delta\rho/^\circ\text{C}$	(40 to 60 °C)	-1.462E-03	$\Delta\rho/\%\text{ void}$	(0.60% to 1.50% void)
$\alpha_{\text{void}} =$	-1.360E-04	$\Delta\rho/^\circ\text{C}$	(60 to 100 °C)	-2.151E-03	$\Delta\rho/\%\text{ void}$	(1.50% to 3.99% void)
All Water						
$\alpha_{\text{water}} =$	3.576E-05	$\Delta\rho/^\circ\text{C}$	(20 to 30 °C)			
$\alpha_{\text{water}} =$	-1.655E-06	$\Delta\rho/^\circ\text{C}$	(30 to 60 °C)			
$\alpha_{\text{water}} =$	-2.809E-05	$\Delta\rho/^\circ\text{C}$	(60 to 100 °C)			
$\alpha_{\text{void}} =$	-5.415E-05	$\Delta\rho/^\circ\text{C}$	(20 to 40 °C)	-1.799E-03	$\Delta\rho/\%\text{ void}$	(0 to 0.60% void)
$\alpha_{\text{void}} =$	-8.968E-05	$\Delta\rho/^\circ\text{C}$	(40 to 60 °C)	-1.913E-03	$\Delta\rho/\%\text{ void}$	(0.60% to 1.50% void)
$\alpha_{\text{void}} =$	-1.307E-04	$\Delta\rho/^\circ\text{C}$	(60 to 100 °C)	-2.068E-03	$\Delta\rho/\%\text{ void}$	(1.50% to 3.99% void)
Fuel Temperature Only						
$\alpha_{\text{fuel}} =$	-9.914E-06	$\Delta\rho/^\circ\text{C}$	(20 to 127 °C)			
$\alpha_{\text{fuel}} =$	-1.387E-05	$\Delta\rho/^\circ\text{C}$	(127 to 227 °C)			
$\alpha_{\text{fuel}} =$	-8.398E-06	$\Delta\rho/^\circ\text{C}$	(227 to 327 °C)			

4.5.4 Operating Conditions

4.5.4.1 PUR-1 HEU Core Power Distribution

Heating tallies were included in the MCNP modeling of the PUR-1 HEU core to evaluate the power profile within the reactor under clean, full-power, critical conditions. Tallies that account for heating due to fission, capture and photon scattering events were utilized. The PUR-1 core is laid out in a 4x4 arrangement, surrounded by graphite reflector blocks. In the HEU core, 13 locations contain 10-plate fuel assemblies, while

two shim rods and one regulating rod can be inserted in the middle of certain assemblies after removing 4 fuel plates. Figure 4-32 shows the HEU core layout modeled in MCNP, and drawings of control and 10-plate fuel assemblies. The numbers in parenthesis in the core layout drawing indicate either the number of fuel plates in the 10-plate fuel assemblies (the remainder are dummy plates of aluminum) or the label of the control assembly (shim or regulating rods).

The heating profile in the PUR-1 was evaluated for five different critical configurations. Table 4-16 compares the heating by bundle for the critical HEU core, with the so-called "50-50-50" rod positions (critical position 3). Heating in non-fueled components was also computed. The total core power was normalized to 1 kW.

The assembly power is highest for position 3-3 in the PUR-1 HEU core. This assembly contains 9 fuel plates and is located in the interior of the core. More important for determining the peak temperatures in the PUR-1 is the plate power. The plate powers shown in Table 4-16 are the average for each bundle in the core. In this case, it is seen that bundle 4-4, which is the location for shim rod SS1, has the highest plate power, so likely the highest temperatures.

Table 4-17 compares the power in individual plates in bundles 4-4 and 3-3 for the reactor control rods at critical position 3. The tallies were summed over the fuel meat in each fuel plate, all clad, coolant, and the bundle can. The plates are numbered from left-to-right in bundle 4-4, and from bottom-to-top in bundle 3-3 (see the bundle drawings in Figure 4-32). It can be seen that plate 262 in bundle 4-4 has the highest power (10.97 W). This plate is adjacent to the large water hole that the SS1 rod falls into, and nearer the center of the reactor than plate 267 on the other side of the water hole.

Figure 4-33 compares the heating tally profiles for the fuel plates in bundle 4-4. Again, the control rods are at critical position 3 in this set of data. The SS1 shim rod is inserted about 10 cm in this reactor model, so the rod tip is in axial segment 13. Consequently, the axial power profile is pushed slightly towards the bottom of the fuel. The results show that plate 262 has the highest peak power of all the plates in bundle. The peak power in plate 89 of bundle 3-3 is about 13% lower than that of plate 262, so there is confidence that plate 262 is the limiting plate for thermal-hydraulic analysis.

Figure 4-34 compares the heating tally profile for plate 262 for each of the critical rod configurations considered. These results confirm that critical position 3 provides the highest peak power in this plate. Lastly, Table 4-18 provides the power for each axial segment plate 262. These data can be used for thermal-hydraulic analysis of the plate.

HEU Core Layout (124 plates)

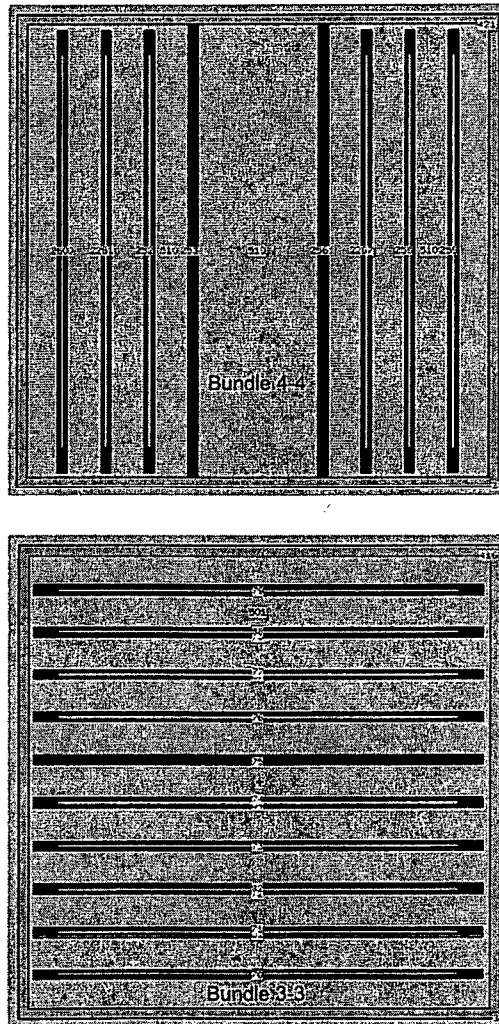


Figure 4-32: PUR-1 HEU Core Layout and Bundle Drawings

Table 4-16: PUR-1 HEU Core Heating Tally Results for Critical Position 3.

Core Component	Power (W)	Plate Power (W)
2-2 (RR)	40.00	6.67
2-3	59.78	7.47
2-4 (SS2)	47.79	7.96
2-5	41.59	5.20
3-2	60.23	7.53
3-3	84.68	9.41
3-4	75.12	9.39
3-5	59.19	7.40
4-2	63.37	7.92
4-3	79.88	9.98
4-4 (SS1)	64.03	10.67
4-5	61.18	7.65
5-2	55.08	6.12
5-3	63.00	7.88
5-4	60.17	7.52
5-5	48.42	6.05
Inter-assembly water	3.71	
Graphite reflector	10.53	
Grid plate	2.52	
Water reflector (pool)	19.23	
SS1	0.29	
SS2	0.22	
RR	0.04	
Total Core Power	1000.00	

Table 4-17: Plate Power Computed from Heating Tallies in Bundles 4-4 and 3-3 in PUR-1 HEU Core.

Bundle 4-4	Power (W)
Plate 260 Meat	10.39
Plate 261 Meat	10.21
Plate 262 Meat	10.97
Plate 267 Meat	10.47
Plate 268 Meat	9.51
Plate 269 Meat	9.39
Clad	0.43
Water	2.38
Can	0.28
Total	64.03
Bundle 3-3	
Plate 80 Meat	8.63
Plate 81 Meat	8.38
Plate 82 Meat	8.38
Plate 83 Meat	8.63
Plate 84 Meat	9.06
Plate 86 Meat	9.33
Plate 87 Meat	9.23
Plate 88 Meat	9.47
Plate 89 Meat	10.22
Clad	0.53
Water	2.52
Can	0.28
Total	84.68

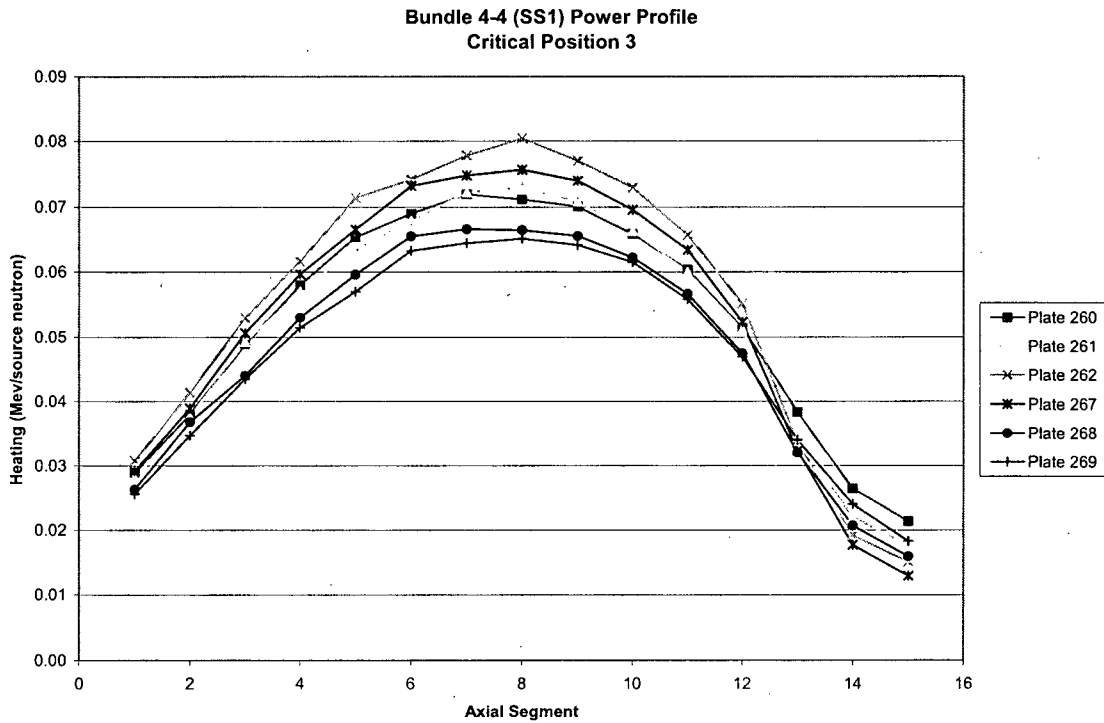


Figure 4-33: Heating Profile in Bundle 4-4 Plates.

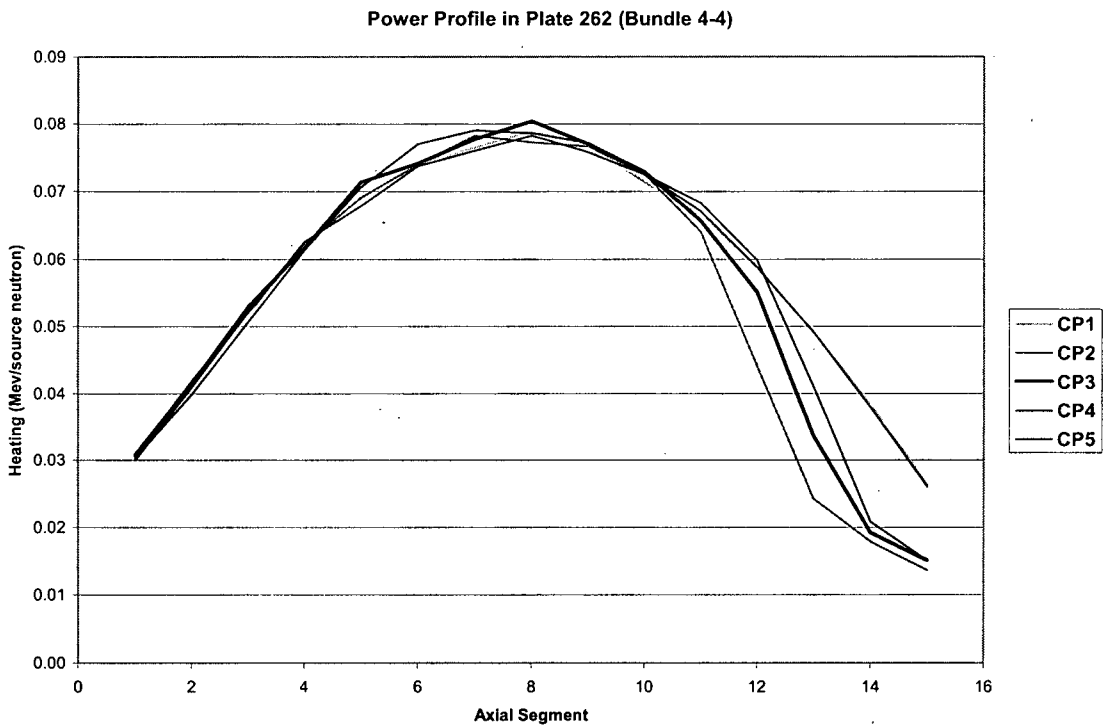


Figure 4-34: Heating Profile in Plate 262 of Assembly 4-4 for Critical Positions

Table 4-18: Axial Heating Profile for Plate 262 of Assembly 4-4 with Critical Position 3 ("50-50-50").

Axial Segment	z-low (cm)	z-high (cm)	Power (W)	σ
1	1.886	5.886	0.41	1.8%
2	5.886	9.887	0.55	1.6%
3	9.887	13.887	0.70	1.4%
4	13.887	17.888	0.82	1.3%
5	17.888	21.888	0.94	1.2%
6	21.888	25.889	0.98	1.2%
7	25.889	29.889	1.03	1.2%
8	29.889	33.890	1.06	1.2%
9	33.890	37.890	1.02	1.2%
10	37.890	41.891	0.96	1.2%
11	41.891	45.891	0.87	1.3%
12	45.891	49.892	0.73	1.4%
13	49.892	53.892	0.45	1.7%
14	53.892	57.893	0.25	2.4%
15	57.893	61.893	0.20	2.7%
Total			10.97	0.4%

4.5.4.2 PUR-1 LEU Core Power Distribution

The new LEU fuel plates will be fabricated with U_3Si_2 dispersion fuel. Each LEU fuel plate will have a nominal loading of 12.5 g U-235, compared with U-235 in the HEU fuel plates. The conversion to LEU fuel requires increasing the assembly fissile loading to compensate for the increased capture in U-238. It is also expected that the boron impurity content of the Al-6061 clad used in fabricating the plates will increase from 10 to 20 ppm. To provide the higher loading, the number of fuel plates/assembly will be increased from 10 HEU plates to 14 LEU plates; this will increase the nominal fuel assembly loading from 165 to 175 g U-235. Likewise, the number of fuel plates in the control locations will be increased from 6 to 8 plates. The overall assembly size will remain the same as for the HEU core, so increasing the number of plates decreases the coolant channel thickness from 5.258 mm to 3.708 mm in the standard fuel bundle, and from 5.258 mm to 5.004 mm for the control bundles.

A fresh LEU-fueled core with 190 fuel plates and 16 “dummy” aluminum plates was evaluated. Figure 4-35 shows the LEU core layout modeled in MCNP, and drawings of control and 14-plate fuel assemblies. The numbers in parenthesis in the core layout drawing indicate either the number of fuel plates in the 14-plate fuel assemblies (the remainder are dummy plates of aluminum) or the label of the control assembly (shim or regulating rods).

The heating profile in the LEU-fueled PUR-1 was evaluated for two different critical core configurations. The rod positions for these configurations were obtained by moving the rods to achieve a calculated excess reactivity near the model bias of 0.32% $\Delta k/k$. For critical position 1, the SS2 rod is positioned at 43 cm above the bottom of the fuel meat, and the SS1 and RR rods are fully withdrawn; the calculated k_{eff} for this configuration is 1.00379 ± 10 pcm. For critical position 2, the SS1 rod is positioned at 48 cm above the bottom of the fuel meat, and the SS2 and RR rods are fully withdrawn; the calculated k_{eff} in this case is 1.00387 ± 9 pcm.

Table 4-19 compares the heating by bundle and in non-fueled components for the LEU core with the rods at critical position 1. The total core power was normalized to 1 kW in this calculation. Critical position 1 was chosen because it yields the highest peak-to-average power density in the LEU core.

The total bundle heating is highest for bundle position 3-3 in the PUR-1 LEU core. This bundle contains 13 fuel plates and is located in the interior of the core. More important for determining the peak temperatures in the PUR-1 is the plate power. The plate powers shown in Table 4-19 are the average for each bundle in the core. In this case, it is seen that bundle 4-4, which is the location for shim rod SS1, has the highest average plate power. It is also observed that bundle 3-4, which is in a grid position that is symmetric with bundle 3-3 relative to the center of the core, has an average plate power that is slightly higher than that in bundle 3-3.

Table 4-20 compares the power in individual plates in bundles 4-4, 3-3, and 3-4 for the reactor with the control rods at critical position 1. The tallies were summed over the fuel meat in each fuel plate, all clad, coolant, and the bundle can. The plates are numbered from left-to-right in bundle 4-4, and from bottom-to-top in bundles 3-3 and 3-4 (see the bundle drawings in Figure 4-35). It can be seen that plate 1348 in bundle 4-4 has the highest power (8.66 W). This plate is adjacent to the large water hole that the

SS1 rod falls into, and nearer the center of the reactor than plate 1355 on the other side of the water hole. Plates 1188 (bundle 3-3) and 1215 (bundle 3-4) face each other across the center-line of the core, and have the same power (6.20 W).

Figure 4-36 compares the local-to-average power density profiles for fuel plates 1188, 1215, and 1348 for the shim rods at critical positions 1 and 2, respectively. Plate 1348 has the highest peak power of all the plates in the LEU core and should be evaluated in the thermal-hydraulics analyses. The “pinching” of the axial power profile when the SS1 shim rod is inserted in critical position 2 is evident. The highest peak/average power density of 2.206 occurs when the rods are in critical position 1.

The power density profiles in plates 1188 and 1215 are nearly identical due to their symmetric positioning. For these two plates, the highest peak/average density (1.586) occurs in plate 1215 with the control rods in critical position 1. The peak power density in plate 1215 is about 28% lower than that of plate 1348. However, the coolant channel width in this standard fuel bundle is narrower than that in the control bundle (3.708 vs. 5.004 mm). Therefore, thermal-hydraulics analyses of both plates 1215 and 1348 with natural convection cooling were performed to determine the temperature profiles.

Photon transport and neutron capture events generate heat in the water and structural components of the PUR-1. For the purposes of thermal-hydraulics analysis of the natural convection cooling of the fuel plates, the direct heating of the water between the fuel plates should be accounted for. This amounts to about 2.25 W in each fuel assembly (see Table 4-20), or 3.5% of the total reactor power.

Neutron reflection at the edges of the fuel plates induces a power density profile along the width of the fuel plates. This is shown in Figure 4-37 for plates 1215 and 1348 with the rods in critical positions 1 and 2. The radial segments are numbered from left-to-right for plate 1215 and from top-to-bottom in plate 1348 (see the plate orientations indicated in Figure 4-35). It is expected that the power density will be higher at the edge of the plate closest to the core center-line. For critical position 1, the SS2 shim rod is inserted in core location 2-4, pushing the power density towards the right edge of plate 1215 even higher. When the SS1 rod is inserted in critical position 2, the opposite effect is observed.

For plate 1348, inserting the SS1 shim rod (critical position 2) has a small effect on the shape of the radial power profile, but reduces the magnitude of the plate power by about 9% compared to the case where only the SS2 shim rod is used for reactor control.

Lastly, Table 4-21 and Table 4-22 provide the axial and radial power profiles for plates 1348 and 1215, respectively. These data are used for thermal-hydraulic analysis of the plate.

Purdue LEU Core Layout (190 plates)

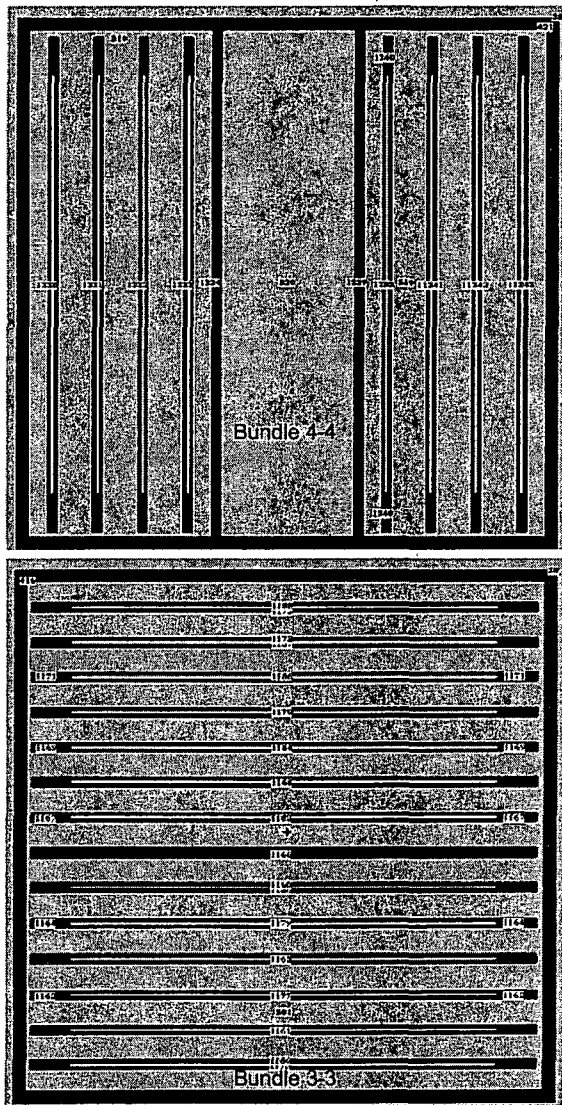


Figure 4-35: PUR-1 LEU Core Layout and Bundle Drawings.

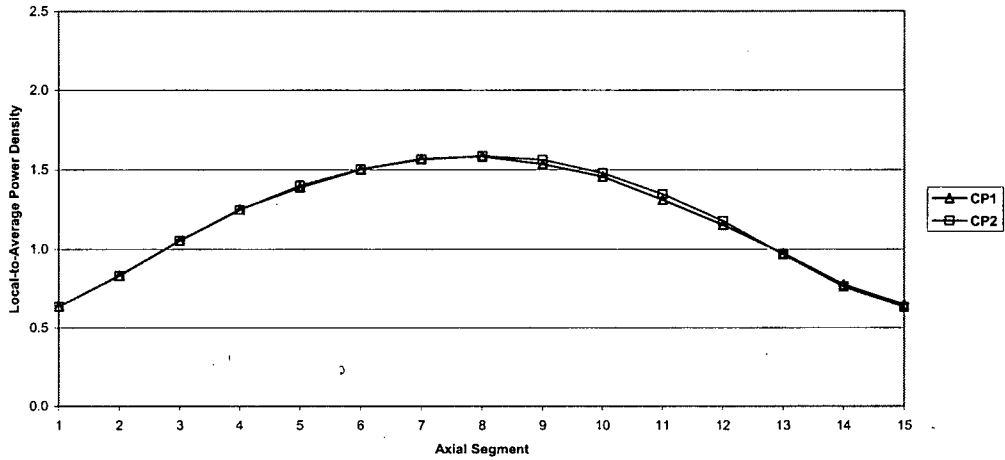
Table 4-19: LEU Bundle Powers Predicted by f7 and f6 Tallies in MCNP.

Bundle or Component	Power (W)	Power (W)
2-2 (RR)	38.66	4.83
2-3	61.88	4.76
2-4 (SS2)	43.28	5.41
2-5	48.90	3.76
3-2	62.33	4.79
3-3	78.20	6.02
3-4	73.02	6.09
3-5	62.31	4.79
4-2	63.88	4.91
4-3	77.32	5.32
4-4 (SS1)	64.38	8.05
4-5	65.07	5.01
5-2	48.69	4.06
5-3	64.39	4.95
5-4	62.83	4.83
5-5	50.99	3.92
Inter-assembly water	3.55	
Graphite reflector	9.56	
Grid plate	2.24	
Water reflector (pool)	18.09	
SS1	0.08	
SS2	0.33	
RR	0.01	
Total	1000.00	

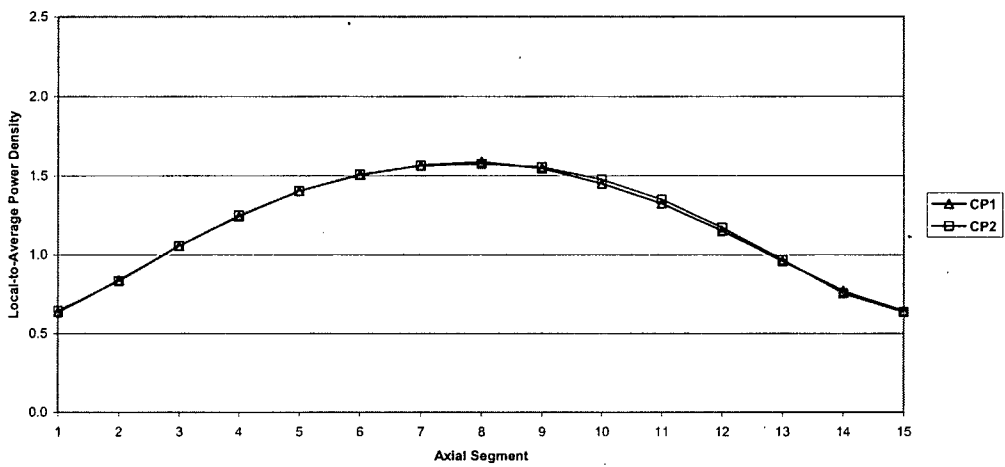
Table 4-20: Plate Power (W) Computed from Heating Tallies in Bundles 4-4, 3-3 and 3-4 in PUR-1 LEU Core with 190 Fuel Plates.

Bundle 4-4	
Plate 1345	7.56
Plate 1346	7.60
Plate 1347	7.93
Plate 1348	8.66
Plate 1355	8.37
Plate 1356	7.51
Plate 1357	7.05
Plate 1358	6.82
Clad	0.37
Water	2.27
Can	0.25
Total	64.38
Bundle 3-3	
Plate 1175	5.62
Plate 1176	5.50
Plate 1177	5.49
Plate 1178	5.55
Plate 1179	5.69
Plate 1180	5.93
Plate 1182	6.01
Plate 1183	5.84
Plate 1184	5.78
Plate 1185	5.79
Plate 1186	5.84
Plate 1187	5.97
Plate 1188	6.20
Clad	0.48
Water	2.24
Can	0.25
Total	78.20
Bundle 3-4	
Plate 1215	6.20
Plate 1216	5.96
Plate 1217	5.83
Plate 1218	5.77
Plate 1219	5.82
Plate 1220	5.98
Plate 1222	5.89
Plate 1223	5.68
Plate 1224	5.60
Plate 1225	5.61
Plate 1226	5.72
Plate 1227	6.01
Clad	0.50
Water	2.21
Can	0.24
Total	73.02

Power Profile (f6:n,p tally) in Plate 1188 (Bundle 3-3)



Power Profile (f6:n,p tally) in Plate 1215 (Bundle 3-4)



Power Profile (f6:n,p tally) in Plate 1348 (Bundle 4-4)

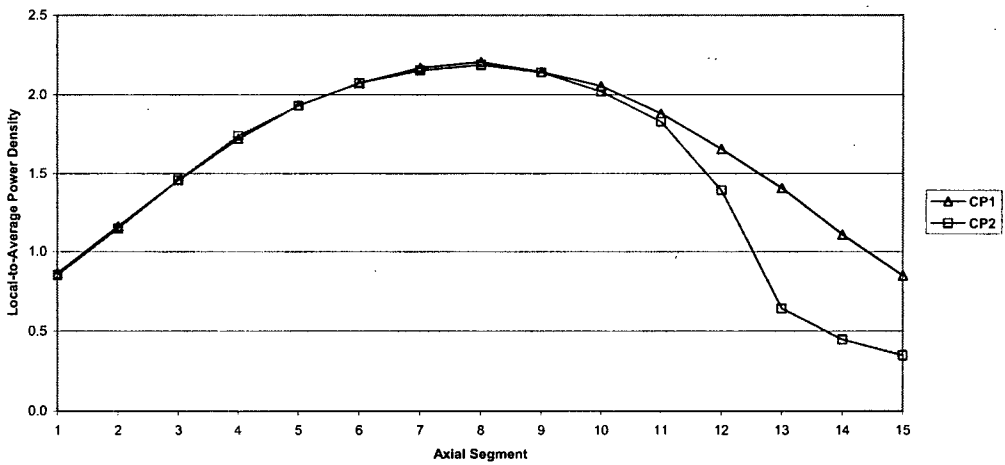
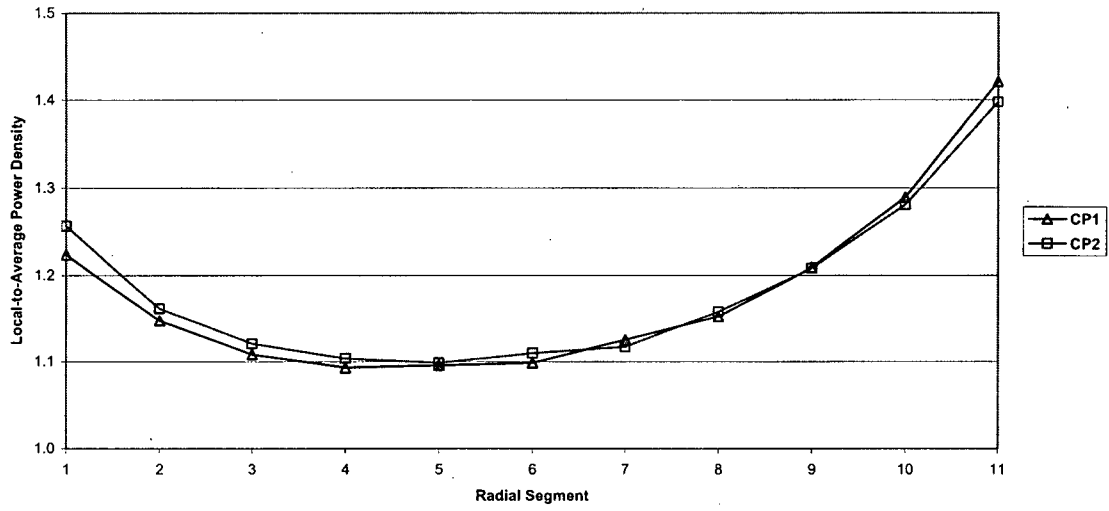


Figure 4-36: Axial Profiles in LEU Plates 1188, 1215 and 1348 for Critical Configurations.

Radial Power Profile (f6:n,p tally) in Plate 1215 (Bundle 3-4)



Radial Power Profile (f6:n,p tally) in Plate 1348 (Bundle 4-4)

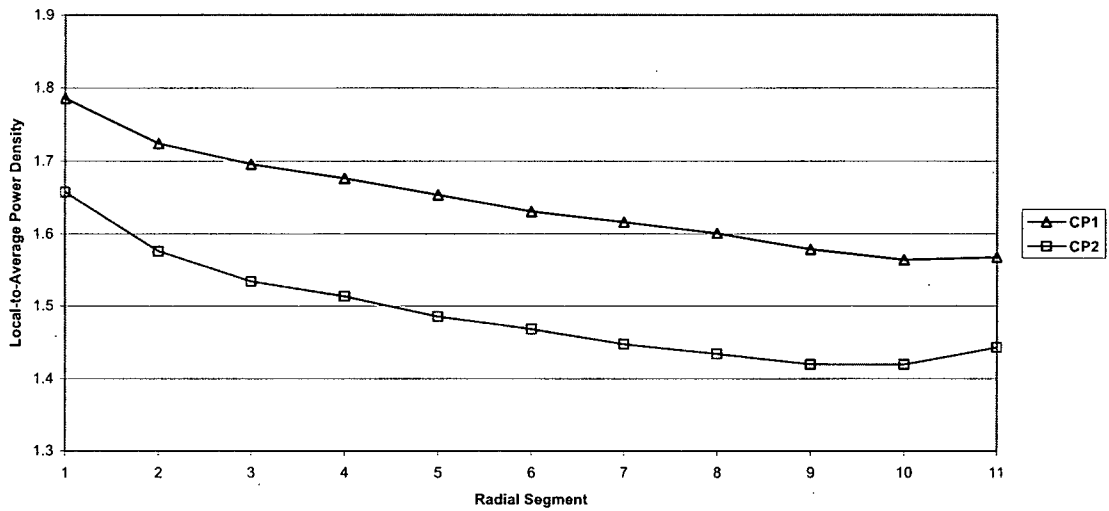


Figure 4-37: Radial Power Profiles in LEU Plates 1215 and 1348 for Critical Configurations

Table 4-21: Axial and Radial Heating Profile (f6:n,p Tally) for LEU Plate 1348 of Bundle 4-4 with Critical Position 1.

Axial Segment	z-low¹ (cm)	z-high¹ (cm)	Power (W)	σ
1	1.886	5.886	0.303	0.51%
2	5.886	9.887	0.407	0.45%
3	9.887	13.887	0.511	0.40%
4	13.887	17.888	0.603	0.37%
5	17.888	21.888	0.678	0.34%
6	21.888	25.889	0.728	0.33%
7	25.889	29.889	0.762	0.32%
8	29.889	33.890	0.774	0.32%
9	33.890	37.890	0.753	0.33%
10	37.890	41.891	0.721	0.34%
11	41.891	45.891	0.659	0.35%
12	45.891	49.892	0.580	0.37%
13	49.892	53.892	0.493	0.40%
14	53.892	57.893	0.389	0.45%
15	57.893	61.893	0.298	0.51%
Total			8.658	0.11%
Radial Segment	y-low¹ (cm)	y-high¹ (cm)	Local/Avg Power Density	σ
1	24.084	24.625	1.786	0.24%
2	24.625	25.167	1.724	0.24%
3	25.167	25.708	1.696	0.24%
4	25.708	26.250	1.676	0.24%
5	26.250	26.791	1.654	0.24%
6	26.791	27.333	1.631	0.25%
7	27.333	27.874	1.617	0.25%
8	27.874	28.416	1.601	0.25%
9	28.416	28.957	1.579	0.25%
10	28.957	29.499	1.564	0.25%
11	29.499	30.040	1.568	0.25%

¹Positions correspond to MCNP model of PUR-1.

Table 4-22: Axial and Radial Heating Profile (f6:n,p Tally for LEU Plate 1215 of Bundle 3-4 with Critical Position 1.

Axial Segment	z-low¹ (cm)	z-high¹ (cm)	Power (W)	σ
1	1.886	5.886	0.223	0.57%
2	5.886	9.887	0.294	0.51%
3	9.887	13.887	0.371	0.45%
4	13.887	17.888	0.436	0.41%
5	17.888	21.888	0.492	0.39%
6	21.888	25.889	0.528	0.38%
7	25.889	29.889	0.550	0.37%
8	29.889	33.890	0.557	0.37%
9	33.890	37.890	0.543	0.37%
10	37.890	41.891	0.508	0.38%
11	41.891	45.891	0.464	0.40%
12	45.891	49.892	0.404	0.43%
13	49.892	53.892	0.337	0.47%
14	53.892	57.893	0.270	0.53%
15	57.893	61.893	0.225	0.57%
Total			6.203	0.12%
Radial Segment	y-low¹ (cm)	y-high¹ (cm)	Local/ Average Power Density	σ
1	24.084	24.625	1.223	0.29%
2	24.625	25.167	1.147	0.29%
3	25.167	25.708	1.108	0.30%
4	25.708	26.250	1.093	0.30%
5	26.250	26.791	1.096	0.30%
6	26.791	27.333	1.099	0.29%
7	27.333	27.874	1.125	0.29%
8	27.874	28.416	1.152	0.29%
9	28.416	28.957	1.209	0.28%
10	28.957	29.499	1.289	0.27%
11	29.499	30.040	1.421	0.27%

¹Positions correspond to MCNP model of PUR-1.

4.6 Functional Design of Reactivity Control Systems

The proposed conversion from HEU fuel to LEU fuel of PUR-1 does not require any changes in the functional design of the reactivity control system. More details about this topic can be found in Reference 1.

4.7 Thermal Hydraulic Characteristics

In this section, the results of the thermal-hydraulic analyses are discussed in order to demonstrate that the PUR-1 LEU core design provides the cooling capacity necessary to ensure fuel integrity under all anticipated reactor operating conditions. Analyses for behavior under hypothetical accident scenarios are presented in Section 13.

4.7.1 NATCON Code Description

Thermal-hydraulic analyses were performed using the computer code NATCON^{8,9}, which can be used to analyze the steady-state thermal-hydraulics of plate type fuel in a research reactor cooled by natural convection. The reactor core is immersed in a pool of water that is assumed to be at a constant average temperature.

NATCON computes coolant flowrate, axial temperatures in the coolant and fuel plate surface and centerline, and the approach to onset of nucleate boiling (ONB). Other safety related parameters such as the Onset of Nucleate Boiling Ratio (ONBR) and Departure from Nucleate Boiling Ratio (DNBR) are calculated as well. And an automatic search for the power at ONB can be performed.

Flow is driven by density differences in the coolant that are the result of coolant heating by the fuel. Resulting buoyant forces are counter-balanced by viscous forces that result from the flow. Hot channel factors may also be introduced for determining safety margins. NATCON v2.0 documentation is included as Appendix 1 of this document. It includes information on the calculation of hot channel factors, inputs, and use of the code.

4.7.2 Fuel Element and Fuel Assembly Geometry

In PUR-1, each fuel plate element is loaded into its own assembly container, or can, as described in Section 4.2.1. Diagrams comparing the relative sizes of the HEU

and LEU standard and control fuel assemblies are shown in Figure 4-38, Figure 4-39 and Figure 4-40.

The primary differences between the HEU and LEU standard fuel elements are the number of plates, the plate spacing, and the outer hardware dimensions. Drawings of the standard elements are shown in Figure 4-38. The HEU and LEU standard elements are loaded into assembly cans made of 6061 aluminum. The HEU assembly cans are to be replaced with new cans of the same design for the LEU assemblies. The cross-section of the HEU and LEU assembly cans with elements inserted is shown in Figure 4-39.



Figure 4-38: Comparison of HEU and LEU Standard Fuel Elements

Figure 4-39: Comparison of HEU and LEU Standard Fuel Assembly

The control fuel assemblies contain two smaller fuel elements which are shown in Figure 4-40. These assemblies are constructed with a channel down the center to provide an insertion space for the control rods. This channel is separated from the fuel element compartments by 6061 aluminum guard plates, which protect the fuel elements from damage when inserting the control rods. Thus, the control fuel elements are contained in their own space.

Figure 4-40: Comparison of HEU and LEU Control Fuel Elements

Two types of channels are encountered in the PUR-1 fuel assemblies. One is the channel between plates, and the other is the channel between the last plate of an element and the assembly can wall. The plate-to-plate channel thickness is fixed by the fuel plate spacers. The plate-to-wall space will be the thickness of the connecting hardware bolt head, assuming that the bolt rests against the assembly can wall. It should be noted that the plate-to-wall channel is heated on only one side, so it can be conservatively assumed that half of the heat from the fuel plate associated with the fuel channel heats the coolant. Table 4-23 summarizes the channel types and thicknesses in PUR-1.

Table 4-23: Channel Types and Thickness in PUR-1 Assemblies

	Plate-to-plate (mils)		Plate-to-wall (mils)	
	Standard	Control	Standard	Control
HEU	207	207	160 ¹	160 ¹
LEU	147	197	79	79

¹ This is the smaller of the two bolt heads on the HEU elements.

In the thermal-hydraulic analyses, the peak power plates identified in section 4.5.4 were analyzed using NATCON. The relative power densities in each fuel plate were obtained from detailed MCNP5 criticality calculations. In the NATCON analysis, the relative axial power profiles of the individual plates were utilized in each respective case.

In the HEU core, the fuel plate with the highest power was plate number 262 in Assembly G-3 (see Figure 4-32), which is adjacent to the control assembly guard plate. As noted above there are two different types of coolant channels associated with the plate. The thermal-hydraulic performance of both channels will be evaluated with NATCON.

In the LEU case, two plates were identified as potentially being the limiting plate. Plate 1348 is in a position similar to plate 262 in the HEU core. The plate-to-plate and plate-to-wall channels will be analyzed for this plate. Plate 1215 is the last plate of standard fuel assembly F-3 (see Figure 4-35). The plate-to-plate channel associated with this plate will be analyzed with NATCON. Because the plate-to-wall thickness for

plate 1215 is the same as for plate 1348, and its plate power is lower, it is not necessary to analyze the plate-to-wall channel.

Hot Channel Factors are used by NATCON to account for dimensional variations inherent in the manufacturing process, as well as variations in other parameters that affect thermal-hydraulic performance. The geometry dimensions used in the NATCON models for the HEU and LEU models are shown in Table 4-24.

Table 4-24: Model Dimensions for the HEU and LEU T-H Models

	HEU		LEU	
Number of Axial Nodes	14		14	
Number of Plates	124		190	
Thermal Conductivity (W/m*K)				
Fuel Meat	143		80	
Clad	180		180	
Pool Temperature (°C)	27		27	
	inches	mm	Inches	mm
Fuel Meat				
Height	23.625	600.05	23.625	600.08
Width	2.468	62.688	2.345	59.563
Thickness	0.020	0.508	0.020	0.508
Channel				
Height	25.110	637.79	25.110	637.79
Width	2.832	71.933	2.832	71.933
Channel Thickness	See Table 4-23.			
Clad Thickness	0.020	0.508	0.015	0.381
Distance assembly can extends above fuel plate	0.450	11.430	0.450	11.430

The hot channel factors that were used in the HEU and LEU cores are shown in Table 4-25 and Table 4-26, respectively. The methodology for determining the hot channel factors and for applying them in NATCON is described in Appendix 1. Values for the tolerance fractions in Tables 4-25 and 4-26 were determined based on data in Reference 5 or engineering judgment.

Based on INL discussions with fuel manufacturer BWXT, the coolant channel thickness is anticipated to have an uncertainty of ± 20 mils. Because of the different types of coolant channels present in PUR-1, multiple tolerance fractions and hot

channel factors are indicated in the tables. The appropriate values were utilized in the NATCON analyses.

Table 4-25: Hot Channel Factors for the HEU Core

Uncertainty	Type of Tolerance	Tolerance Fraction	Hot Channel Factors		
			FBULK Coolant Temp. Rise	FFILM Film Temp Rise	FFLUX Heat Flux
Fuel meat thickness	Random	0.050	1.000	1.050	1.050
U-235 Homogeneity	Random	0.030	1.000	1.030	1.030
U-235 Mass per plate	Random	0.030	1.015	1.030	1.030
Power Density	Random	0.100	1.049	1.100	1.100
Channel Thickness	Random	0.097 ¹ 0.125 ²	1.165 ¹ 1.222 ²	1.097 ¹ 1.125 ²	1.000
Flow Distribution	Random	0.200	1.200	1.000	1.000
Random Uncertainties	Combined		1.312¹ 1.361²	1.154¹ 1.173²	1.120
Power Measurement F_Q	Systemic		1.500		
Flow friction factor F_w	Systemic		1.000		
Heat Transfer Coeff. F_H	Systemic		1.200		
1. Plate-to-plate channel. 20 mil uncertainty on 207 mil channel thickness. 2. Plate-to-wall channel. 20 mil uncertainty on 160 mil channel thickness.					

Table 4-26: Hot Channel Factors for the LEU core

Uncertainty	Type of Tolerance	Tolerance Fraction	Hot Channel Factors		
			FBULK Coolant Temp. Rise	FFILM Film Temp Rise	FFLUX Heat Flux
Fuel meat thickness	Random	0.000	1.000	1.000	1.000
U-235 Homogeneity	Random	0.200	1.000	1.200	1.200
U-235 Mass per plate	Random	0.030	1.015	1.030	1.030
Power Density	Random	0.100	1.049	1.100	1.100
Channel Thickness	Random	0.102 ¹	1.175 ¹	1.102 ¹	1.000
		0.137 ²	1.247 ²	1.137 ²	
		0.253 ³	1.549 ³	1.253 ³	
Flow Distribution	Random	0.200	1.200	1.000	1.000
Random Uncertainties	Combined		1.321 ¹	1.248 ¹	1.226
			1.384 ²	1.264 ²	
			1.679 ³	1.339 ³	
Power Measurement F _Q	Systemic		1.500		
Flow friction factor F _w	Systemic		1.000		
Heat Transfer Coeff. F _H	Systemic		1.200		
1. Plate-to-plate channel. 20 mil uncertainty on 197 mil channel thickness. 2. Plate-to-plate channel. 20 mil uncertainty on 146 mil channel thickness. 3. Plate-to-wall channel. 20 mil uncertainty on 79 mil channel thickness.					

4.7.3 Thermal Hydraulic Analysis Results

The NATCON/ANL V 2.0 code was used to determine the thermal-hydraulics performance of the PUR-1. First, the code was used to compute the power at which the ONB is reached for the plates being examined in each of the HEU and LEU cores. This was done to identify the limiting channel. Then the limiting channel was evaluated under nominal operating conditions for both the HEU and LEU cores. The ONB results provide verification that the Safety Limit (SL) and Limiting Safety System Settings (LSSS, trip points) of the Technical Specifications will indeed assure safe operation of PUR-1 for the LEU core.

4.7.3.1 NATCON Analyses

The reactor pool temperature varies throughout the year from about 22°C to 27°C depending on the ambient temperature and humidity conditions in the reactor room. In all of the following calculations, the higher value 27°C was used.

The power search function of NATCON was used to determine the power level at the Onset of Nucleate Boiling for both the HEU and LEU cores. Table 4-27 provides a summary of the ONB powers for each of the cases analyzed. For the HEU core, the limiting channel/plate was the plate-to-plate (P-T-P) case, with an ONB power of 76.3 kW. For the LEU core, the limiting channel/plate was plate 1348 with the plate-to-plate channel, which had an ONB power of 96.1 kW.

Table 4-27: ONB Powers for HEU and LEU Cores

	HEU Plate 262		LEU Plate 1348		LEU Plate 1215
Channel Type	P-T-P ¹	P-T-W ²	P-T-P	P-T-W	P-T-P
ONB Power (kW)	76.3	149.5	96.1	187.8	165.6
1. Plate-to-Plate spacing					
2. Plate-to-Wall spacing					

Using NATCON, the thermal-hydraulics parameters of the HEU and LEU cores at the nominal operating conditions were also calculated. All hot channel factors are included in these calculations. These results are shown in Table 4-28.

Table 4-28: 1 kW Operating Conditions for PUR-1 as Determined by NATCON

	HEU (Plate 262) P-T-P	LEU (Plate 1348) P-T-P
Max. Fuel Temp. (°C)	29.6	29.6
Max. Clad Temp. (°C)	29.6	29.6
Coolant Inlet Temp. (°C)	27.0	27.0
Coolant Outlet Temp. (°C)	28.7	29.3
Margin to incipient boiling (°C)	81.1	81.2
Coolant Velocity (mm/s)	6.04	5.11
Coolant Mass Flow Rate (kg/s)	0.0028	0.0018

4.7.3.2 Safety Limits for the LEU Core

In PUR-1, the first and principal physical barrier protecting against the release of radioactivity is the cladding of the fuel plates. The 6061 aluminum alloy cladding has an incipient melting temperature of 582 °C. However, measurements (NUREG 1313, Ref. 4) on irradiated fuel plates have shown that fission products are first released near the blister temperature (~550 °C) of the cladding. To ensure that the blister temperature is never reached, NUREG-1537 (Ref. 11) concludes that 530 °C is an acceptable fuel and cladding temperature limit not to be exceeded under any conditions of operation. As a result, PUR-1 has proposed a safety limit in its Technical Specifications requiring that the fuel and cladding temperatures should not exceed 530 °C.

4.7.3.3 Limiting Safety System Settings for the LEU Core

Limiting safety system settings (LSSS) for nuclear reactors are settings for automatic protective devices related to those variables having significant safety functions. When a limiting safety system setting is specified for a variable on which a safety limit have been placed, the setting must be chosen such that the automatic protective actions will correct the abnormal situation before a safety limit is reached. Table 4-29 shows the maximum power, the LSSS and operating power for PUR-1.

Table 4-29: Key Power Levels for Reactor Operation and LSSS for PUR-1

Maximum Power Level Including 50% Uncertainty	1.8 kW
Limiting Safety System Settings Power Level	1.2 kW
Operating Power Level	1.0 kW

During steady-state operation, peak clad temperatures are maintained far below 530°C , as well as below the temperatures required for ONB (see Table 4-28). NATCON was used to determine the minimum power for ONB for the HEU and LEU cores in the limiting channels, as well as the thermal-hydraulic parameters at these calculated powers. The results of these calculations are shown in Table 4-30.

Table 4-30: Power Levels at the Onset of Nucleate Boiling for HEU and LEU Cores.

	HEU	LEU

Power level at ONB (kW)	76.3	96.1
Max. Fuel Temp. (°C)	112.6	112.6
Max. Clad Temp. (°C)	112.5	112.5
Coolant Inlet Temp. (°C)	27.0	27.0
Coolant Outlet Temp. (°C)	41.4	42.6
Onset of Nucleate Boiling Ratio	1.0	1.0
Coolant Velocity (mm/s)	55.3	53.3
Coolant Mass Flow Rate (kg/s)	0.021	0.019

The licensed operating power level of PUR-1 is 1 kW. The LSSS scram setting of 120% power (1.2 kW) is well below the power level of 76.3 in the HEU core and 96.1 kW in the LEU core, at which ONB would occur in the respective limiting channels. Thus, the present LSSS on power at 1.2 kW (120% power) will protect the reactor fuel and cladding from reaching the Safety Limit under steady state operations.

Chapter 13 (Accident Analyses) analyzes two hypothetical transients based on values of the Technical Specifications for the LEU core. These transients are: (1) Rapid insertion of the maximum reactivity worth of 0.3% $\Delta k/k$ of all moveable and non-secured experiments, and (2) Slow insertion of reactivity at the maximum allowed rate of 0.04% $\Delta k/(k*s)$ due to control blade withdrawal.

For the case of the rapid insertion, of 0.3% $\Delta k/k$, the reactor scram was initiated based on the power level trip, assuming failure of the period trip. For the case of the slow insertion of 0.04% $\Delta k/(k*s)$, scram was initiated on the second power level trip, assuming the first power level trip failed. The reason for this is that the period trip is never reached for the case of this slow reactivity insertion.

Thus the selected LSSS is a conservative setting which ensures that the maximum fuel and cladding temperatures do not reach the safety limit of 530 °C for the range of accident scenarios that were analyzed. In summary, the selected LSSS will protect the reactor fuel and cladding from reaching the safety limit of 530°C under any condition of operation.

5 REACTOR COOLANT SYSTEM

The conversion of PUR-1 from HEU to LEU fuel does not require any changes to the reactor coolant system. More details about this topic can be found in Reference 1.

6 ENGINEERED SAFETY FEATURES

The conversion of PUR-1 from HEU fuel to LEU fuel does not require any changes to the engineered safety systems.

7 INSTRUMENTATION AND CONTROL SYSTEMS

No changes to the instrumentation and control (I&C) systems are proposed or required by the conversion of PUR-1 from HEU to LEU fuel.

8 ELECTRICAL POWER SYSTEMS

No changes to the electrical power systems are required by the conversion of HEU to LEU fuel for PUR-1.

9 AUXILIARY SYSTEMS

9.1 Systems Summary

No changes to the Auxiliary systems are required by the conversion of PUR-1 from HEU to LEU fuel.

9.2 Ventilation System

No changes to the confinement ventilation system are proposed or required for the conversion of PUR-1 from HEU to LEU fuel. The new LEU fuel will be operationally similar to the HEU fuel, and existing ventilation capabilities are adequate.

9.3 Heating and Air Conditioning Systems

No changes to the confinement heating and air conditioning systems are proposed or required by the conversion of PUR-1 from HEU to LEU fuel. The new LEU fuel will be operationally similar to the HEU fuel, and existing air conditioning and heating capacities are adequate.

9.4 Fuel Element Handling and Storage

Existing procedures will be used for fuel element handling and storage. No changes are necessary as a result of the conversion from HEU to LEU. The storage of the extra LEU plates will be in a secure, dry location. Parametric eigenvalue calculations were performed with MCNP5, varying the storage plate spacing in a

hypothetical flooded condition to ensure that a critical configuration could not be achieved. These results are shown in Figure 9-1. The maximum k-eff obtained in these calculations was 0.41, which is less than the Technical Specification (TS 5.3.1) requirement of less than 0.8 (see Ref. 2).

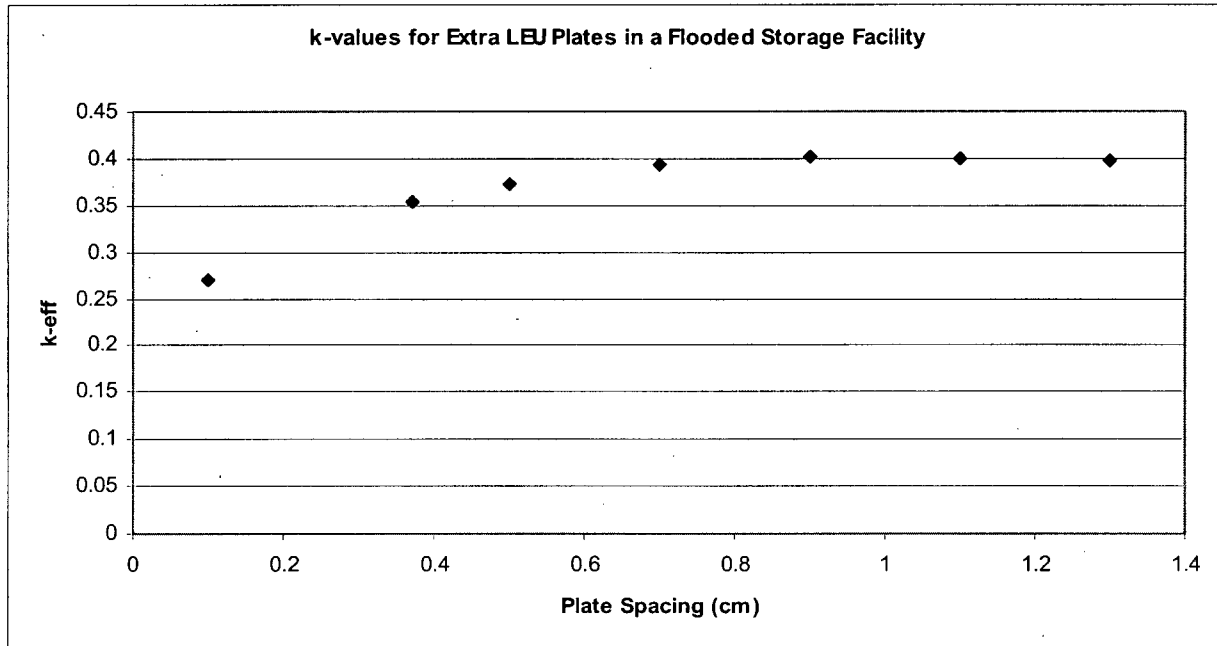


Figure 9-1: k-eff Values for Flooded Condition of Fuel Storage Facility.

9.5 Other Auxiliary Systems

No other auxiliary systems as listed in Chapter 9 of NUREG 1537 will be affected by the conversion of PUR-1 from HEU to LEU.

10 EXPERIMENTAL FACILITIES AND UTILIZATION

No changes to experimental facilities or utilization are required by the conversion of PUR-1 from HEU to LEU fuel.

11 RADIATION PROTECTION PROGRAMS AND WASTE MANAGEMENT

The conversion of PUR-1 from HEU to LEU does not require any changes to the radiation protection and radioactive waste management of the facility. More details about this topic can be found in Reference 1.

12 CONDUCT OF OPERATIONS

12.1 Organization and Staff Qualification

The HEU to LEU conversion does not require any changes to the organization and staff qualification of PUR-1 personnel. More details about this can be found in References 1 and 2.

12.2 Procedures

PUR-1 staff proposes to revise the core reload and approach to critical procedure, in order to utilize additional data made possible by this analysis, and new technology available since the previous procedure (Procedure 95-4-A) was written.

PUR-1 staff proposes to revise Procedure 95-5, "Standard Procedure for Inspection of Fuel Plates" to "Standard Procedure for Inspection of Fuel Assemblies." See the revisions to Technical Specifications in Section 14.

12.3 Operator Training and Requalification

The conversion from HEU to LEU fuel requires minor changes to the requalification and training program for operators. Some modifications will be required where fuel description, loading and safety limits are addressed, and operators will be made aware of any changes. Modified procedures will become part of the training documentation as necessary.

12.4 Emergency Plan

The only changes to the Emergency Plan for PUR-1 required by the conversion of PUR-1 from HEU to LEU fuel will be in the description of the facility, Section 1.4. "93% enriched" will be replaced with "19.75% enriched."

12.5 Physical Security Plan

Any changes to the facility physical security plan required by the conversion will be submitted under separate cover and withheld from public disclosure.

12.6 Reload and Startup Plan

The core reload and approach to critical procedure has been modified to utilize the information developed in these analyses, and to take advantage of new technology

in the process. This procedure is shown in "Appendix 2: New Core loading procedure", on Page 89.

13 ACCIDENT ANALYSIS

Four hypothetical accident scenarios are addressed: The Maximum Hypothetical Accident (MHA), Rapid Addition of Reactivity Accident, Reduction in Cooling Accident, and another accident involving the slow insertion of reactivity due to control rod withdrawal.

13.1 Maximum Hypothetical Accident

The maximum hypothetical accident (MHA), failure of a fueled experiment (see Ref. 1), does not involve the reactor fuel. Therefore, the conversion of PUR-1 from HEU to LEU fuel will not affect the MHA, and is not analyzed here.

13.2 Rapid Addition of Reactivity Accident

The analyses of this transient utilizes the reactor physics and reactivity coefficients determined by MCNP5 as described in Chapter 4, and thermal-hydraulic parameters determined by NATCON as described in Chapter 4, and the PARET/ANL¹⁰ code.

The original PARET code has been adapted by the Reduced Enrichment for Research and Test Reactors (RERTR) Program to provide transient and thermal-hydraulics analysis for research and test reactors with both plate and pin-type fuel assemblies. The PARET/ANL version of the code has been subjected to extensive comparisons with the SPERT I and SPERT II (light and heavy water) experiments. These comparisons were quite favorable for a wide range of transients up to and including melting of the clad. Revisions of the code include new and more appropriate heat transfer, departure from nucleate boiling (DNB) and flow instability correlations, improved edits, reactor trips, control insertion model, a decay heat power model, and a loss of flow model.

The rapid insertion of the maximum worth of moveable and unsecured experiments (0.3% $\Delta k/k$) as specified by the Technical Specifications was evaluated. An assumption was made that the period trip (7s) failed, and scram was initiated on the power trip at 1.2kW. Since the assumed measurement uncertainty on core power is

50%, a core power trip setting of 1.8 kW was utilized in the accident calculation. A delay of 0.1 seconds from the sending of scram signal to beginning of control rod motion is assumed. Fuel/coolant channels that are representative of the hottest fuel plates (as identified in section 4.7) were modeled in the PARET analyses.

Results of this transient are summarized in Table 13-1. The reactor power increases from 1 kW to the trip setting of 1.8 kW in less than 2.5 seconds. There is a negligible increase in the clad temperature as a result of this hypothetical accident. The safety limit is never in danger of being reached.

Table 13-1: Transient Results for Rapid Insertion of 0.3% $\Delta k/k$ for PUR-1.

Core	P_o (kW)	P_{max} (kW)	Time of Peak Power (s)	$T_{clad,max}$ (°C)	
				@ t=0	Maximum
HEU	1.000	1.810	2.5	28.59	28.59
LEU	1.000	1.807	2.5	28.93	29.38

These results demonstrate the ability of the LSSS to protect the safety limit of fuel temperatures not to exceed 530°C. The maximum temperatures achieved in the fuel are well below temperature of incipient boiling as well. Therefore PUR-1 can maintain the fuel integrity during this accident scenario.

13.3 Reduction in Cooling Accidents

The PUR-1 SAR (Ref. 1) evaluated a loss-of-coolant accident during full-power operation. Due to the construction of the reactor pool, the possibility of sudden LOCA by unintentional drainage is extremely unlikely. Furthermore, if the pool drained instantaneously while the reactor was operating, the loss of moderator would shut down the reactor.

In Reference 1, the fuel temperature rise in the HEU core was estimated to be 9.5 °C assuming adiabatic conditions for 24 hours after a hypothetical LOCA. A similar temperature rise that is far below the safety limit of 530°C is also expected for the LEU core.

13.4 Other Accidents

The other accident examined was the inadvertent removal of the control rod of maximum worth, or the "runaway rod." This accident assumes a stuck switch on the control rod of highest worth (SS-1) while the rod is being raised starting from the 1 kW full power level. The period trip is not reached in this accident, and it is assumed that the first power trip fails. The reactor is then scrammed on the redundant LSSS power trip. Allowing for a power level measurement uncertainty of 50%, the 1.2 kW trip level is actually 1.8 kW.

A calculation was done for a slow insertion of 0.04% $\Delta k/k/s$. Results are presented in Table 13-2. The clad temperature climbed less than 3°C as a result of this accident. The resulting clad temperatures are much less than the temperature of incipient boiling, and well under the safety limit of 530°C.

The maximum reactivity insertion rate from the withdrawal of the SS-1 control rod is 0.009% $\Delta k/k/s$ and 0.018% $\Delta k/k/s$ for the HEU and LEU cores, respectively. These values are both below the reactivity insertion rate used in this hypothetical accident analysis. Thus, the results for the runaway rod transient analyzed here demonstrate the protection of the safety limit by the limiting safety system setting.

Table 13-2: Transient Results for Slow Insertion of 0.04% $\Delta k/k/s$ for PUR-1.

Core	P _o (kW)	P _{max} (kW)	Time of Peak Power (s)	T _{clad,max} (°C)	
				@ t=0	Maximum
HEU	1.000	1.825	6.000	29.03	31.90
LEU	1.000	1.814	6.000	28.93	29.38

14 TECHNICAL SPECIFICATIONS

For the conversion of PUR-1 from HEU to LEU fuel, PUR-1 staff proposes the following changes to the Technical Specifications.

Safety Limit (T.S. 2.1)

The Safety Limit Technical Specification, Section 2.1, from the present Technical Specifications (Ref. 2) reads as follows:

2.1 Safety Limit

Applicability - This specification applies to the steady state power level.

Objective - The objective is to define a power level below which it can be predicted with confidence that no damage to the fuel elements will occur.

Specification - The true value of the instantaneous power of the reactor shall not exceed 50 kW.

Basis - The Purdue University Reactor utilizes fuel of the same type as is used in several similar reactors, such as the reactor at the University of Missouri, Rolla. These reactors use natural convection cooling and are routinely operated at power levels exceeding 50 kW with no apparent damage to the fuel.

The steady state power of 50 kW was chosen because calculations indicate that the average heat flux from fuel into coolant would be less than 0.5 watts/cm, and that no boiling would occur at this level. With fuel plate temperatures associated with this power level no damage to the fuel elements will occur. The aluminum alloy cladding does not melt below 1100 °F and is expected to maintain its integrity and retain essentially all of the fission fragments at temperatures below 1100 °F. For a step input of reactivity equal to the available excess in the core, combined with a postulated failure of the scram mechanisms such that all control rods jam out of the core, it is estimated that the coolant temperature would rise to less than 130 °F. This coolant temperature would restrict cladding temperatures well below 1100 °F thus assuring retention of all fission fragments.

The proposed change to the Safety Limit Technical Specification reads as follows:

2.1 Safety Limit

Safety limits for nuclear reactors are limits upon important process variables that are necessary to reasonably protect the integrity of certain of the physical barriers that guard against the uncontrolled release of radioactivity. The principal physical barrier is the fuel cladding.

Applicability - This specification applies to the temperature of the reactor fuel and cladding under any condition of operation.

Objective - The objective is to ensure fuel cladding integrity.

Specification - The fuel and cladding temperatures shall not exceed 530 °C (986 °F).

Basis - In the Purdue University Reactor, the first and principal barrier protecting against release of radioactivity is the cladding of the fuel plates. The 6061 aluminum alloy cladding of the LEU fuel plates has an incipient melting temperature of 582 °C. However, measurements (NUREG-1313⁴) on irradiated fuel plates have shown that fission products are first released near the blister temperature (~550 °C) of the cladding. To ensure that the blister temperature is never reached, NUREG-1537¹¹ concludes that 530 °C is an acceptable fuel and cladding temperature limit not to be exceeded under any condition of operation.

Limiting Safety System Setting (T.S. 2.2)

The PUR-1 proposes to modify the basis of the Limiting Safety System Setting (LSSS) Technical Specification (TS 2.2, pages 7-8, Ref. 2).

The present LSSS Technical Specification reads as follows:

2.1 Limiting Safety System Setting (LSSS)

Applicability - This specification applies to the reactor power level safety system setting for steady state operation.

Objective - The objective is to assure that the safety limit is not exceeded.

Specification - The measured value of the power level scram shall be no higher than 1.2 kW.

Basis - The LSSS has been chosen to assure that the reactor protective system will be actuated in such a manner as to prevent the safety limit from being exceeded during the most severe expected abnormal condition.

The safety margin between LSSS and the SL is sufficient to assure that the peak power achieved in a transient, starting at 1 kW with a 1-second period and terminated by dropping a control rod, will not exceed 50 kW. The 1-second period corresponds to a reactivity of .006 $\Delta k/k$, which is the maximum authorized to be loaded into the reactor.

The safety margin that is provided between the LSSS and the SL also allows for instrument uncertainties associated with measuring the above parameter.

2.1 Limiting Safety System Setting

Applicability - This specification applies to the reactor power level safety system setting for steady state operation.

Objective - The objective is to assure that the safety limit is not exceeded.

Specification - The measured value of the power level scram shall be no higher than 1.2 kW.

Basis - The LSSS has been chosen to assure that the **automatic** reactor protective system will be actuated in such a manner as to prevent the safety limit from being exceeded during the most severe expected abnormal condition.

The function of the LSSS is to prevent the temperature of the reactor fuel and cladding from reaching the safety limit under any condition of operation. During steady-state operation, a power level of 96.7 kW is required to initiate the onset of nucleate boiling. This is far larger than the maximum power of 1.8 kW, which allows for 50% instrument uncertainties in measuring power level.

For the transients that were analyzed, the temperature of the fuel and cladding reach maximum temperatures of 31°C, assuming reactor trip at 1.8 kW after failure of the first trip. This temperature is far below the safety limit of 530°C.

Containment

The PUR-1 staff proposes to revise Technical Specification 4.4.d, describing the requirement to inspect representative fuel plates annually should be removed. Based on 44 years of operating experience, and excellent control of pool water chemistry, no corrosion has been observed in fuel plates or assemblies. No new alloys will be introduced into the reactor as a result of conversion from HEU to LEU fuel. The LEU plates are planned to have boehmite surface which will enhance their resistance to corrosion.

In order to maintain ALARA doses to reactor staff, and to limit exposure of the LEU fuel plates to mechanical damage from handling, it is proposed that the Technical

Specification 4.4.d, which reads: "Representative fuel plates shall be inspected annually, with no interval to exceed 15 months;" be changed to "Representative fuel assemblies shall be inspected annually, with no interval to exceed 15 months."

Fuel Assemblies

Technical Specification 5.2, "Fuel Assemblies," describes the design features of PUR-1 fuel. Specifications 5.2.1, 5.2.2, and 5.2.3 should be changed to reflect the new fuel design. They should read as follows:

- 5.2.1 The fuel assemblies shall be MTR type consisting of aluminum clad plates containing uranium enriched to approximately 19.75% in the U-235 isotope.
- 5.2.2 A standard fuel assembly shall consist a maximum of 14 fuel plates containing up to 185 ± 8.75 grams of U-235.
- 5.2.3 A control fuel assembly shall consist of a maximum of 8 fuel plates containing up to 105 ± 5 grams of U-235.

15 OTHER LICENSE CONSIDERATIONS

15.1 Prior Utilization of Reactor Components

The conversion of PUR-1 from HEU to newly manufactured LEU fuel assemblies. There are no prior use issues with the conversion.

15.2 License Conditions

The HEU core will not be kept at this facility after the conversion is completed, therefore no changes to the license are necessary. Possession of both the HEU and LEU cores for the duration of the conversion process is expected to be permitted by the order to convert, and no modifications to possession limits are required.

15.3 Decommissioning

The conversion of PUR-1 from HEU to LEU has no effect on the decommissioning plan of PUR-1, as established in the previous license extension (See Ref. 4).

APPENDIX 1: NATCON DOCUMENTATION

NATCON Code Running Instructions (July 22, 2006)

1. UNIX command to run NATCON: `executable_filename < input_filename`
`/home/sol1a/kalimull/natcon/natconlf95.x < input_filename`
2. Output file name: NATCON.PRINT
3. Figure 1 shows the geometry input data and the natural circulation flow circuit that are modeled in the code.
4. The correspondence between hot channel factors used in NATCON and E. E. Feldman's hot channel factors is shown on the next page.
5. The code analyzes a **single coolant channel**, including the effect of hot channel factors. The channel gets heated by a single fuel plate (actually, by the heat generated in half a plate on each side of the channel). The older NATCON code version 1.0 uses three hot channel factors. The new version 2.0 uses six hot channel factors, as described below.
6. Standard and control assemblies mentioned in the input data are treated alike in the code.
7. Corrections:
 - (i) The last equation on page 2 in the code documentation [ANL/RERTR/TM-12] is incorrect, which is now corrected. The error is not important because it affected only the fuel center-line temperature which is usually not very different from cladding surface temperature.
 - (ii) The frictional pressure drop in *all* the unheated plate length, CHANHT-FUELHT, is computed assuming the coolant to be at pool temperature. This should be calculated assuming lower half of the unheated length at pool temperature, and the upper half at the channel exit temperature. This is not yet corrected.
8. Power in hot plate = $Q_{PLATE} = FQ * R_{PEAK} * C_{PWR} / N_{PLATE}$, where
 $N_{PLATE} = \text{Total number of plates in standard and control subassemblies}$
 $= N_{STDEL} * N_{PLTSE} + N_{CONEL} * N_{PLTCE}$

9. The spreadsheet for computing six hot channel factors, developed by E. E. Feldman, from the uncertainties/tolerances of 9 engineering quantities is good for forced flow only (laminar or turbulent). It is not applicable to natural circulation. For natural circulation, a recently developed Fortran program is described below to find the six hot channel factors. The relationships between bulk coolant temperature rise, reactor power and the power-induced flow rate, needed by the program, are also developed below.

1. Hot Channel Factors in the NATCON Code Version 1.0

NATCON code version 1.0 [Ref. ANL/RERTR/TM-12] uses three hot channel factors (FQ, FW, FH). Using the source code and documentation, the factor FH used in NATCON is found to be the same as the factor FNUSLT used by E. E. Feldman. Table 1 shows the engineering uncertainties included in each of the six hot channel factors used by E. E. Feldman. The correspondence between NATCON hot channel factors and E. E. Feldman's six hot channel factors is as follows.

<u>Feldman's Hot Channel Factor</u>		<u>NATCON Input Variable</u>
<i>System-wide Factors:</i>		
FFLOW	a factor to account for the uncertainty in total reactor flow	FW (approximately)
FPOWER	a factor to account for the uncertainty in total reactor power	FQ
FNUSLT	a factor to account for the uncertainty in Nu number correlation	FH
<i>Local Factors:</i>		
FBULK	a hot channel factor for local bulk coolant temperature rise	FBULK (new input)
FFILM	a hot channel factor for local temperature rise across the coolant film	FFILM (new input)
FFLUX	a hot channel factor for local heat flux from cladding surface	FFLUX (new input)

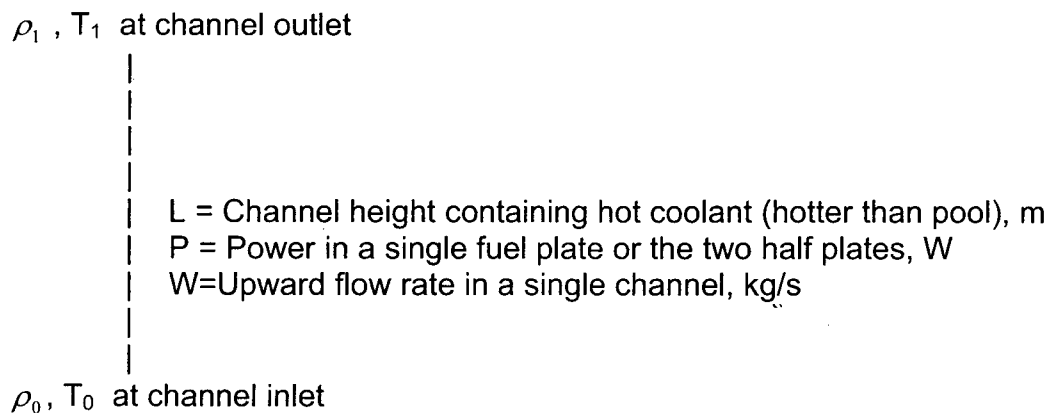
2. Hot Channel Factors in the NATCON Code Version 2.0

Sections 2.1 and 2.2 develop two thermal-hydraulic relationships that are used in section 2.3 to obtain formulas for the hot channel factors from user-supplied manufacturing tolerances and measurement uncertainties.

2.1 Flow Rate in a Coolant Channel versus Power of a Fuel Plate

NATCON is a laminar natural circulation code. The flow rate is calculated in the code by balancing the buoyancy pressure force to the laminar friction pressure drop. Following this concept, an analytical relationship is developed here (with some approximation) for the coolant flow rate in a single coolant channel in terms of the power generated in a fuel plate and the channel geometrical dimensions. The analytical relationship is needed for obtaining hot channel factors.

The hot channel factor FW used in the code to account for the uncertainty in coolant flow rate is actually applied to the laminar friction factor in the code, that is, the laminar friction factor is multiplied by FW^2 . It is not applied directly to the flow rate. The relationship developed here explains how this technique works.



Schematic of what the code analyses, that is, a single rectangular coolant channel heated by a half of a fuel plate on each side (right and left sides).

The above schematic shows what the code analyses, that is, a single rectangular coolant channel heated by a half of a fuel plate on each side (right and left sides). See Fig. 1 for details. The buoyancy pressure force is caused by the decrease in water

density due to heating in the channel. The temperature dependence of water density can be written as

$$\rho(T) = \rho_0 - \rho_0 \beta (T - T_0) \quad (1)$$

where

- T_0 = Water temperature at channel inlet, C
- T_1 = Water temperature at channel outlet, C
- ΔT = $T_1 - T_0$ = Temperature rise in channel from inlet to outlet, C
- ρ_0 = Water density at channel inlet, i.e., the water density in the pool, kg/m^3
- β = Volumetric expansion coefficient of water, per C
- $\bar{\rho}$ = Average coolant density in the channel, kg/m^3
- L = Channel height that contains hotter coolant (hotter than pool), m. It is the sum of heat generating length of fuel plate, non-heat generating fuel plate length at top, and the assembly duct length above the top of fuel plate
- g = Acceleration due to gravity, 9.8 m/s^2

The buoyancy pressure force is given by

$$\text{Buoyancy } \Delta p = (\rho_0 - \bar{\rho}) g L \quad (2)$$

The average coolant density $\bar{\rho}$ is given by

$$\bar{\rho} = 0.5 (\rho_0 + \rho_1) = \rho_0 - 0.5 \rho_0 \beta (T_1 - T_0) = \rho_0 - 0.5 \rho_0 \beta \Delta T \quad (3)$$

$$\text{Buoyancy } \Delta p = 0.5 \rho_0 \beta \Delta T g L \quad (4)$$

The coolant temperature rise ΔT can be written in terms of the input power P generated in a fuel plate, as shown by Eq. (5) below, and then the buoyancy Δp of Eq. (4) can be written in terms of the input power P , as shown by Eq. (6).

$$\Delta T = P / (W C_p) \quad (5)$$

$$\text{Buoyancy } \Delta p = \frac{\rho_0 \beta g L P}{2 W C_p} \quad (6)$$

Ignoring the minor losses at channel inlet and outlet, the laminar frictional pressure drop in the channel is written below as Eq. (9) after using the laminar friction factor given by Eq. (7), and after replacing the coolant velocity by mass flow rate using Eq. (8). The

parameter C in Eq. (7) is a constant for a given channel cross section, but it depends upon the channel cross section aspect ratio width/thickness, and varies from 57 for aspect ratio 1.0 (square channel) to 96 for an infinite aspect ratio (infinitely wide channel).

$$f = C / R_e \quad (7)$$

$$W = \bar{\rho} A V \quad (8)$$

$$\text{Frictional } \Delta p = \frac{\bar{\rho} f L_c V^2}{2D} = \frac{C \bar{\mu} L_c W}{2 \bar{\rho} A D^2} \quad (9)$$

where

- f = Moody friction factor for laminar flow in the channel
- R_e = Reynolds number in the channel = $\bar{\rho} V D / \bar{\mu}$
- A = Flow area of the channel cross section, m²
- D = Equivalent hydraulic diameter of the channel cross section, m
- L_c = Total coolant channel length causing frictional pressure drop, m.
- V = Coolant velocity averaged over the channel cross section, m/s
- W = Coolant mass flow rate in the channel, kg/s
- μ(T) = Temperature-dependent dynamic viscosity of water, N-s/m²
- $\bar{\mu}$ = Average coolant dynamic viscosity in the channel, N-s/m²

The code equates the frictional Δp of Eq. (9) to the buoyancy Δp of Eq. (6) to find the steady-state coolant flow rate W in the channel, as shown in Eq. (10) below. Equation (10) can be rewritten as Eq. (11).

$$\frac{\rho_0 \beta g L P}{2 W C_p} = \frac{C \bar{\mu} L_c W}{2 \bar{\rho} A D^2} \quad (10)$$

$$W^2 = \frac{\rho_0 \bar{\rho} A D^2 \beta g L P}{C \bar{\mu} L_c C_p} \quad (11)$$

Equation (11) is the main result. All parameters in this equation are constant except $\bar{\mu}$, $\bar{\rho}$, and the parameter C in the laminar friction factor. Based on Eq.(11), the relationship between the flow rate W and these three parameters is given by Eq. (12) below.

$$W \propto \sqrt{\frac{\bar{\rho}}{C \bar{\mu}}} \quad (12)$$

Equation (12) shows that if the friction factor parameter C is multiplied by the square of an input hot channel factor FW, the flow rate W will be reduced approximately by the factor FW. How good this approximation will be depends upon the sensitivity of the coolant kinematic viscosity ($\bar{\mu} / \bar{\rho}$) to temperature.

2.2 Bulk Coolant Temperature Rise versus Power of a Fuel Plate

Equation (5) expresses, for laminar natural circulation, the bulk coolant temperature rise in terms of fuel plate power, coolant flow rate and specific heat. Putting the value of flow rate obtained in Eq. (11) into Eq. (5), the bulk coolant temperature rise is given by Eq. (13) below, purely in terms of power and the geometrical dimensions of the channel. The right hand side of Eq. (13) is rearranged into two factors in Eq. (14), such that the second factor is sensitive to power and channel geometrical dimensions that usually have manufacturing tolerances and measurement uncertainties, and the first factor is insensitive to power and channel geometrical dimensions.

$$\Delta T = \left(\frac{C \bar{\mu} L_c P}{C_p \rho_0 \bar{\rho} A D^2 \beta g L} \right)^{1/2} \quad (13)$$

$$\Delta T = \left(\frac{C \bar{\mu} L_c}{C_p \rho_0 \bar{\rho} \beta g L} \right)^{1/2} \left(\frac{P}{A D^2} \right)^{1/2} \quad (14)$$

The nominal flow area and hydraulic diameter of a rectangular coolant channel are given by

$$A = t_{nc} w_{nc} \quad (15)$$

$$P_w = 2 (t_{nc} + w_{nc}) \quad (16)$$

$$D = 4 A / P_w = 2 t_{nc} w_{nc} / (t_{nc} + w_{nc}) \quad (17)$$

where

t_c = Channel thickness (spacing between fuel plates), m

t_{nc} = Nominal channel thickness (spacing between fuel plates), m

t_{hc} = Minimum channel thickness in hot channel (spacing between fuel plates), m

- w_c = Channel width, assumed not to change from its nominal value, m
 P_w = Wetted perimeter of the nominal channel, m
 P_{nc} = Power generated in a fuel plate, without applying manufacturing tolerances, W
 P_{hc} = Power generated in a fuel plate, after applying manufacturing tolerances, W

Because the channel thickness t_c is much smaller than the channel width w_c in most experimental reactors, Eq. (17) reduces to

$$D \approx 2 t_c \quad (18)$$

Using the channel area and hydraulic diameter given by Eqs. (15) and (18) into Eq. (14), the bulk coolant temperature rise can be written in terms of power, channel thickness, and channel width. This is the desired relationship for use in finding hot channel factors.

$$\Delta T = \left(\frac{C \bar{\mu} L_C}{C_P \rho_0 \bar{\rho} \beta g L} \right)^{1/2} \left(\frac{P}{4 w_c t_c^3} \right)^{1/2} \quad (19)$$

2.3 Formulas for Hot Channel Factors

For use in NATCON version 2.0 code, six hot channel factors (three global/systemic and three local/random) are obtained from 9 manufacturing tolerances and measurement uncertainties u_1, u_2, \dots, u_9 that are defined below. These are fractional uncertainties rather than percent. Of these nine uncertainties, those affecting a particular hot channel factor are indicated in Table 1. The systemic hot channel factors are given by Eqs. (20) through (22), and the random hot channel factors are given by Eqs. (23) through (25). A utility computer program NATCON_HCF has also been developed to compute the hot channel factors using these formulas.

$$FQ = 1 + u_7 \quad (20)$$

$$FW = 1 + u_8 \quad (21)$$

$$FH = 1 + u_9 \quad (22)$$

The ratio of the power generated in hot plate to its nominal power, caused by the uncertainties in neutronics-computed power and in U-235 mass per plate, can be written as

$$\frac{P_{hc}}{P_{nc}} = (1 + u_1)(1 + u_2) \quad (23)$$

The ratio of bulk coolant temperature rise in hot channel to the temperature rise in the nominal channel, caused by the uncertainties in neutronics-computed power, U-235 mass per plate, and channel thickness, is obtained from Eq. (19). Only the quantity in the second parentheses is important here because the quantity in the first parentheses is insensitive to these uncertainties.

$$\frac{\Delta T_{hc}}{\Delta T_{nc}} = \left(\frac{P_{hc}}{P_{nc}} \right)^{1/2} \left(\frac{t_{nc}}{t_{hc}} \right)^{3/2} = (1+u_1)^{1/2} (1+u_2)^{1/2} \left(\frac{1}{1-u_5} \right)^{3/2} \quad (24)$$

The uncertainty in flow distribution is assumed to reduce the channel flow to $(1-u_6)$ times the flow without this uncertainty, and therefore the bulk coolant temperature rise is increased by the factor $(1+u_6)$. This uncertainty in bulk coolant temperature rise is statistically combined with that given by Eq. (24) to obtain the following formula for the hot channel factor FBULK for input to NATCON version 2.0 code.

$$FBULK = 1 + \sqrt{\left\{ (1+u_1)^{1/2} (1+u_2)^{1/2} \left(\frac{1}{1-u_5} \right)^{3/2} - 1 \right\}^2 + u_6^2} \quad (25)$$

The temperature drop across coolant film on the cladding surface at an axial location is given by Eq. (26). Here the heat flux q'' (W/m^2) on the cladding surface is replaced by $t_f q'''/2$ in terms of the volumetric power density q''' (W/m^3) in the fuel meat.

$$\Delta T_{film} = \frac{q''}{h} = \frac{t_f q'''}{2h} \quad (26)$$

The convective heat transfer coefficient h (W/m^2-C) is given by Eq. (27). Here the laminar Nusselt number N_u is independent of flow rate, and varies only slowly with the aspect ratio (width/thickness) of coolant channel. The main variation of the heat transfer coefficient with channel thickness is due to the denominator of Eq. (27). The numerator of Eq. (27) is considered to be constant.

$$h = \frac{N_u K_{cool}}{D} = \frac{N_u K_{cool}}{2 t_c} \quad (27)$$

Using Eq. (27) for the heat transfer coefficient, the temperature drop across coolant film can be written as Eq. (28).

$$\Delta T_{film} = \frac{q''' t_f t_c}{N_u K_{cool}} \quad (28)$$

Equation (28) states that ΔT_{film} is directly proportional to the fuel meat thickness (having uncertainty u_3), the channel thickness (having uncertainty u_5), and the power density in meat. The uncertainty in power density is caused by three uncertainties, that is, u_1 , u_2 and u_4 . Statistically combining these five uncertainties gives the following formula for the hot channel factor FFILM for input to NATCON version 2.0 code.

$$FFILM = 1 + \sqrt{u_1^2 + u_2^2 + u_3^2 + u_4^2 + u_5^2} \quad (29)$$

The temperature drop from fuel meat centerline to cladding surface is given by Eq. (30). Here the heat flux q'' through the cladding has been replaced by $t_f q'''/2$ in terms of the power density q''' in the fuel meat.

$$\Delta T_{metal} = T_{max} - T_{wall} = \frac{t_{fuel} q'''}{2} \left(\frac{t_{fuel}}{4K_{fuel}} + \frac{t_{clad}}{K_{clad}} \right) \quad (30)$$

The expression within the parenthesis on the right hand side of Eq. (30) varies slowly compared to the heat flux $t_{fuel} q'''/2$. Therefore, the ratio of the temperature drop from meat centerline to cladding surface in hot channel to that in the nominal channel is given by Eq. (31), and this ratio is the hot channel factor FFLUX for input NATCON version 2.0 code.

$$FFLUX = \frac{\Delta T_{metal, hc}}{\Delta T_{metal, nc}} = \frac{(t_{fuel} q''')_{hc}}{(t_{fuel} q''')_{nc}} \quad (31)$$

In Eq. (31), the uncertainty in power density is caused by three uncertainties, that is, u_1 , u_2 and u_4 . The uncertainty in the meat thickness is given by u_3 . Statistically combining these four uncertainties gives the following formula for the hot channel factor FFLUX for input to NATCON version 2.0 code.

$$FFLUX = 1 + \sqrt{u_1^2 + u_2^2 + u_3^2 + u_4^2} \quad (32)$$

where

- u_1 = Fractional uncertainty in neutronics calculation of power in a plate
- u_2 = Fractional uncertainty in U-235 mass per plate = $\Delta m / M$
- u_3 = Fractional uncertainty in local (at an axial position) fuel meat thickness

- u₄ = Fractional uncertainty in U-235 local (at an axial position) homogeneity
- u₅ = Fractional uncertainty in coolant channel thickness = $(t_{nc} - t_{hc}) / t_{nc}$
- u₆ = Fractional uncertainty in flow distribution among channels
- u₇ = Fractional uncertainty in reactor power measurement
- u₈ = Fractional uncertainty in flow due to uncertainty in friction factor
- u₉ = Fractional uncertainty in convective heat transfer coefficient, or in the Nu number correlation
- M = Nominal mass of U-235 per plate, gram
- Δm = Tolerance allowed in U-235 mass per plate, gram

Input Description of NATCON Code Version 2.0 of July 22, 2006

Card 0: Title card of 80 characters

FORMAT (A80)

Card 1: Major input options

FORMAT (8I6)

NN Number of axial heat transfer nodes in the fueled height of fuel plate (maximum 20); number of node boundaries = NN+1

NTRANC = 1 Include entrance effects in heat transfer coefficient
 = 0 Ignore entrance effects. Assume fully developed heat transfer coefficient

NSTDEL Number of standard subassemblies (also called standard elements)

NPLSE Number of fuel plates in a standard subassembly

NCONEL Number of control subassemblies (also called control elements)

NPLTCE Number of fuel plates in a control assembly

IPRT If non-zero, debugging output will be printed.

IONB = 1 Use Bergles and Rohsenow correlation for onset of nucleate boiling (ONB), (Recommended)
 = 0 Use the Ohio State University correlation for onset of nucleate boiling if $\rho V t_{CH} / \mu < 700$ and $T_W \geq T_{SAT}$;

Otherwise, use Bergles and Rohsenow correlation; where

ρ = Coolant density
 μ = Coolant dynamic viscosity
 V = Coolant velocity
 t_{CH} = Coolant channel thickness
 T_W = Cladding wall temperature
 T_{SAT} = Coolant saturation temperature

Card 2: Fuel plate geometry and thermal conductivity

FORMAT (6E12.5)

FUELHT Axial length of fuel meat in a plate, m
FUELWT Width of fuel meat in a plate, m
FUELTK Thickness of fuel meat in a plate, m
FUELK Thermal conductivity of fuel meat, W/m-C
CLADTK Cladding thickness, m
CLADK Thermal conductivity of cladding, W/m-C

Card 3: Coolant channel geometry and pool temperature (see Fig. 1)

FORMAT (6E12.5)

CHANHT Coolant channel height (total height of a plate, i.e., fueled + unfueled height), m
CHANWT Coolant channel width, m
CHANTK Coolant channel thickness (spacing between plates), m
DEPTH Distance from coolant pool free surface to the bottom of coolant channel, m
CHIMNY Unheated section of the assembly (also called element) above fuel plates, m
TPOOL Average temperature coolant pool, C

Card 4: Convergence Criterion, Radial power factor, Nominal Reactor Power

FORMAT (4E12.5)

- DELTA Criterion for convergence criterion of frictional and buoyant forces (per unit channel cross-sectional area) to the same value, N/m^2 (Recommended $1.0E-6$)
- VGUESS Initial guess for coolant inlet velocity, m/s; A guess 100 times off is acceptable.
- RPEAK Radial power peaking factor, that is, the factor by which this channel's power differs from the average channel.
- CPWR Nominal reactor power level, *if desired*, kW. If this input is zero or omitted, then the code will search the nominal power level at which the ONB ratio is 1.0 *with all six hot channel factors applied*.

Card 5: Hot Channel Factors

FORMAT (6E12.5)

System-wide Factors:

- FW A factor to account for uncertainty in total reactor flow due to uncertainty in friction factor.
Note: The flow will be reduced by this factor approximately. This is because FW^2 is actually used as a multiplier for friction factor and minor loss coefficients. The friction factor $f = C/Re$ where C is 58 to 96 depending upon the width/thickness ratio of the coolant channel.
- FQ A factor to account for uncertainty in total reactor power measurement.
*Note: The natural convection flow rate in the coolant channel is induced by the power $FQ * RPEAK * (Average Power per Plate)$.*
- FH A factor to account for uncertainty in Nu number correlation, or convective heat transfer coefficient correlation.

Local Factors:

- FBULK Hot channel factor for local bulk coolant temperature rise

FFILM Hot channel factor for local temperature rise across the coolant film

FFLUX Hot channel factor for local heat flux from cladding surface

Card 6: Axial Power Shape in the fueled region of the plate, input at interfaces of heat transfer nodes, NN+1 pairs

FORMAT (2E12.5)

(ZR(I), QVZ(I), I=1, NN+1)

ZR(I) Height at the lower end of axial node I, measured from the bottom of the fuel meat, normalized such that the total height of the meat in a fuel plate is 1.0. ZR(1) is zero and ZR(NN+1), the upper end of node NN, equals 1.0.

QVZ(I) Normalized power density at the lower end of axial node I

Table 1. Uncertainties Included in the Six Hot Channel Factors Used in NATCON Version 2.0 (X implies that an uncertainty affects a hot channel factor)

Uncertainty Fraction		FQ	FW	FH	FBULK	FFILM	FFLUX
Local or random uncertainties							
1	Neutronics calculation of power in a plate, u_1				X	X	X
2	U-235 mass per plate, u_2				X	X	X
3	Local fuel meat thickness, u_3					X	X
4	U-235 axial homogeneity, u_4					X	X
5	Coolant channel thickness, u_5				X ¹	X	
6	Flow distribution among channels, u_6				X	X	
System-wide uncertainties							
7	Reactor power measurement uncertainty, u_7	X					
8	Flow uncertainty due to uncertainty in friction factor, u_8		X				
9	Heat transfer coefficient uncertainty due to uncertainty in Nu number correlation, u_9			X			

Note 1: Bulk coolant temperature rise $\Delta T = P / (W C_p)$. Equation (11) is used to find the change in flow W due to a reduced channel thickness.

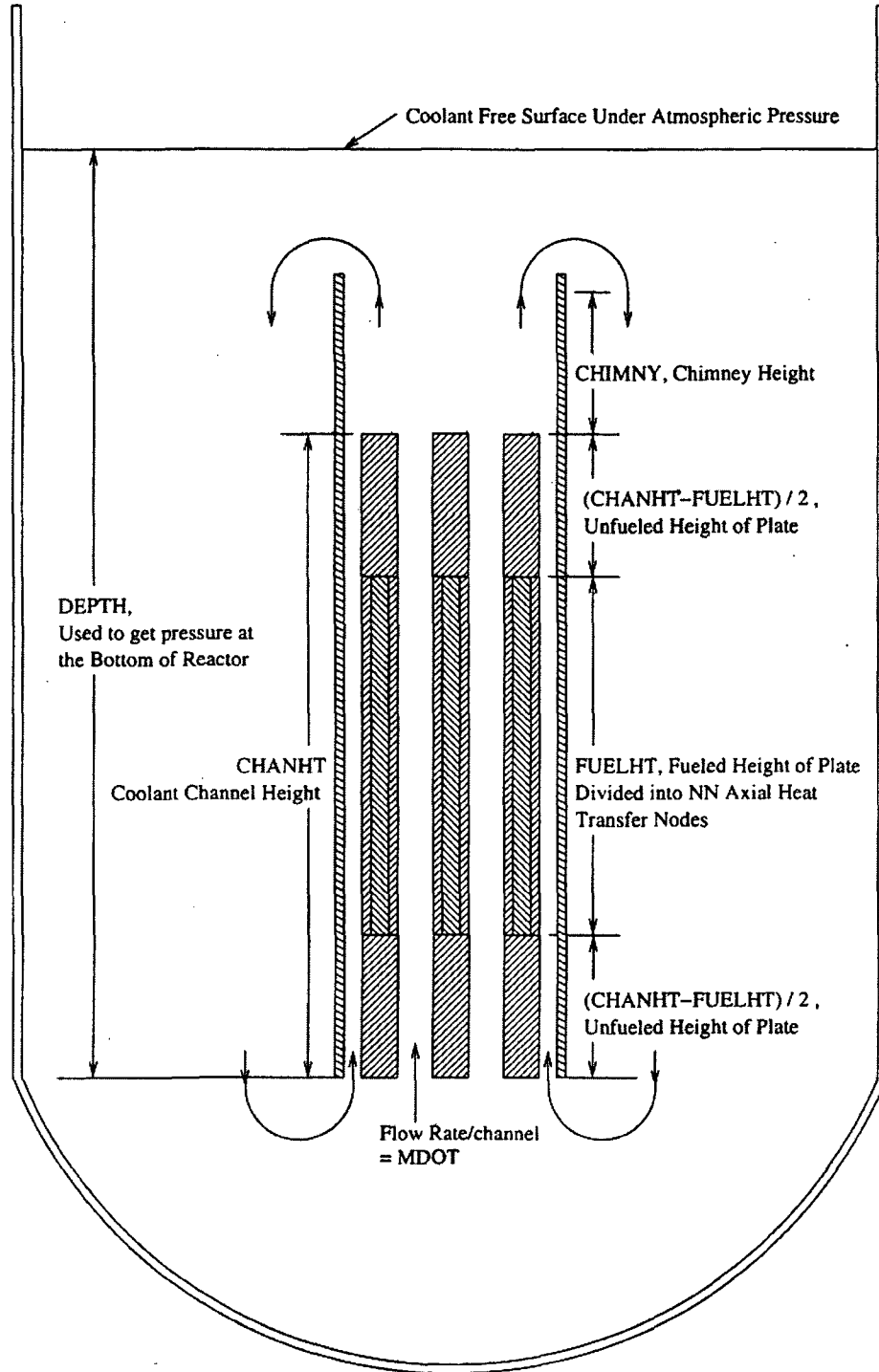


Figure 1: Reactor Geometry and Natural Circulation Coolant Flow Circuit Modeled in NATCON Code.

APPENDIX 2: NEW CORE LOADING PROCEDURE (DRAFT)

Procedure 06-1-CL

Standard Procedure for Core Loading

Purpose

The purpose of this procedure is to provide a series of steps for the safe assembly of the PUR-1 core. This version of the procedure may be used to assemble a new core, or also for cores exceeding any reassembly specifications in Procedure 95-4-A (or other procedure), or when a plate-by-plate loading is required or specified. The guiding considerations of this procedure are:

1. To ensure a safe procedure for the assembly of fuel into the reactor array (core) so that an uncontrolled critical mass will not be assembled.
2. To ensure that the maximum excess reactivity, defined as the reactivity in the core when all of the fuel has been inserted and the control rods are raised to their upper limits, does not exceed $0.006 \Delta k/k$.

Limits

The Tech. Spec. excess reactivity limit (T.S. 3.1.d) for the PUR-1 core is $0.006 \Delta k/k$ (3.1.d.). The administrative limit is $0.005 \Delta k/k$ (0.003 to $0.005 \Delta k/k$). Also (T.S. 6.1.12) during fuel changes and movement of large bulk experiments, an SRO will be present in the reactor room.

Summary

This procedure provides a step by step method for assembling a core of 'almost' unknown loading. The 'almost' in the above line makes reference to the 'code' to be run as a part of step 1 in the Initial Conditions section below. This procedure may be used in conjunction with Procedure 95-4-A 'Standard Procedure for the Disassembly and Reassembly of the PUR-1 Reactor Core' if at any step of 95-4-A fails to meet the statistical requirements during reloading, cores that have an excess reactivity, $\rho_{ex} > 0.005$ but $< 0.006 \Delta k/k$, or if equipment fails, or the 36 hour time limit cannot be met as required in 95-4-A. This procedure may be used if for any reason a 'full approach' to the critical loading is required.

This procedure is intended to achieve a critical mass right at, or very near the upper limit of the control rods motion. Then it allows subsequent plate adjustments to adjust the excess reactivity.

Plate-by-plate loadings: It will not be considered a violation of this procedure if as a part of any other procedure (Example Procedure 95-4-A) steps are omitted. Example steps 1-5 and step 7 may be omitted but step 6 may be included. The SRO must decide what steps are to be used. Graphs, and extrapolations must be done and steps or the intent of steps should be followed as closely as possible.

Graphs: Several graphs or their calculated equivalent are required during the assembly:

Graph Name	
[LL-Ch-1] and [LL-AUX]	Lower limit (LL) graph, these should not predict critical with the expected fuel loading. (Required)
[Shim-CH-1] and [Shim-AUX]	Lower limit of the shim range, these should not predict critical with the expected fuel loading. (Required)
[50-CH-1] and [50-AUX]	(Recommended) Normal critical banked rod height.
[UL-CH-1] and [UL-AUX]	Upper limit (UL) of rod motion, these graphs should be the first to predict critical. (Required)
[# of plates CH-1] and [# of plates AUX]	Plot of $1/M$ vs. rod height. This graph is used to predict critical as the rods are raised from (LL) through shim range and on to (UL). (Required)

Note on [# of plates CH-1] and [# of plates AUX]: These graphs will be used when the rods are raised to predict the critical rod height. Each time plates are added (a single loading step), the previous graphs are set aside and two new graphs [# of plates CH-1] are generated, with C_0 being the counts at (LL). $1/M$ is plotted at shim range (SR), 50cm, and possibly (UL). It is intended that each graph would be labeled as to the actual number of plates in the core as: "14 plates CH-1", but the plates, step number, date and time may help to identify the graph if it is necessary to refer to them later.

It will not be a violation of this procedure if extra graphs are generated or extra data points are taken on any graph (i.e. stops at 45cm or 55cm etc.).

Core Loading: After the initial loading (source, FC, SS1, SS2, RR and unfueled reflectors), only experimental data will be used for further core loading. As to the actual loading, calculated models 'codes' may be used for checking, not for the loading of fuel. Data taken during the actual experiment is the only data to be used for the prediction of the loading not precalculated data. The reciprocal of the measured neutron multiplication 'One over M' ($1/M$) calculations, and the graphs $1/M$ vs. fuel loading (total plate count) are required for this procedure. Core load predictions will be made using a minimum of two detectors. The predictions will use straight line extrapolations from the last two data points. Data from the most conservative detector extrapolation will be used for core loading. No single loading step will exceed one-half of the most conservative experimentally predicted critical loading. After the initial loading, the maximum single loading step will be one fuel element. The minimum loading will be one plate. After the initial loading, both shim safety rods must be 'cocked' (i.e. scramable and withdrawn to at least the lower limit of the shim range) before any fuel element may be added.

Dummy plates are allowed in any assembly (i.e. element). Plate positions of known dummies may be filled with aluminum dummy plates unless it is necessary to add an additional fuel plate to meet the final loading conditions of excess reactivity. Then, dummy plate position/s may be filled with fuel plate/s or vice versa.

Data: Extrapolations are required for any 'core load prediction' prior to the addition of fuel. These extrapolations are typically plotted by hand; it will not be considered a violation of this procedure if the extrapolations are done by hand or the use of any other computing device. It will be necessary to 'take data' (take counts, calculate C_0/C , plot, and extrapolate the $1/M$ line) with the rods at the lower limit, shim range (≈ 40 cm), and upper limit. It is recommended that counts also be taken at 50 cm (i.e. the predicted final critical rod position). If data from either the lower limit or shim range extrapolate and indicate a critical loading will be achieved on any addition, the next addition may not be added without consulting an SRO. Data at the rod heights of upper limit (UL) and 50 cm data will not be taken once critical is predicted at these rod heights.

Excess Reactivity: The unofficial excess reactivity may be estimated during a run at the end of this procedure using a previous rod worth from the old core. The reported

excess reactivity will require rod calibrations for the new core and will not be immediately available at the completion of this procedure. It will not be considered a violation of this procedure if plate adjustment(s) are required at a later date.

After criticality is achieved, the excess reactivity is adjusted to a value between 0.003 and 0.005 $\Delta k/k$ by adding individual plates to any element.

Notes on Taking Counts: When k approaches 1.0 it will be necessary to wait a minimum of three minutes after any reactivity change (i.e. the addition of a fuel element or the movement of rods) before starting a count. When k is far from 1.0 any counts may be started after waiting only a few seconds.

Note: Operators may gain a feel for k and the time to wait between counts by watching Channel 3 'the linear channel'. Observe that Channel 3 will level fast when k is far from 1.0 and slowly near 1.0. As some counts are at LL and some are at SR and UL so too k could be 'far from' and 'close to' 1.0 during one fuel loading.

Adjust the counting time(s) for a minimum of 4000 counts for each recorded reading or sum successive counts from the same detector. If readings from two detectors are not consistent, counts may be repeated and or any count time may be adjusted. Operators may find it helpful to watch Channel 3 'the linear channel' to look for count rate level or counting inconsistencies.

Five minute counts are recommended. If counts of other times are used it will be necessary to adjust the counts to keep all data consistent.

Criticality: Operators should take great care when raising the rods between fuel additions as this is a point where criticality may be reached unexpectedly. The SRO must watch as fuel is added. Watch for a critical (linear increase) or supercritical rise on Channel 3, also period, or any other indication(s) of criticality. If Channel 3 (or any other criticality indication) increases slowly and does not seem to be leveling in less than 5 minutes at SR or LL, lower the rods to the LL, or remove fuel, and do not proceed without the SRO's knowledge.

Securing the Reactor: As this is a long procedure, it may not be possible to complete the entire loading in one day. The reactor may be secured for the night or weekend in the usual manner, the fuel handling tool must also be secured at the close of the shift. Meet the initial conditions prior to continuing this procedure or after any 4 hour delay.

Prestart note: If the procedure is delayed due to any reason the source or detectors should not be moved during the prestart checkout before the next operation.

Fuel Inventory: During all fuel movements and any loading we are required to maintain a complete fuel inventory of fuel plate serial numbers, plate orientations, fuel assembly numbers, handle color coding, handle orientation, the locations on all fuel and installed dummies. This may be done with the help of a loading board.

Log Book: Log as much of the raw data, calculations, extrapolations, estimates, plate loadings, serial numbers, orientations, observations and etc. as this can help future core work.

Initial Conditions

1. A 'code' (computer program) for the purpose of calculating; the fuel loading, and excess reactivity, of the reactor; must have been tested, run, and approved by at least one of the reactor senior staff (i.e. Laboratory Director, or Reactor Supervisor). Backup code runs by an outside lab (such as Argon National Lab) or another NRC approved lab or agency are currently required before an initial core loading.

Exception: This procedure may be used without a code run for any subsequent loading such as: Loading adjustments of up to 14 plates, relocating any or all dummies, installing new regulating rods, reflector changes, or anytime a plate-by-plate loading of a previously loaded core is required.

2. Install an auxiliary (AUX) neutron detector, with associated counting system, outside of the reflector and on the side of the core opposite from the neutron source. It will not be considered a violation of this procedure if more than one auxiliary detector is installed in any location.
3. An SRO is required to move the actual fuel or remove a control rod.
4. A minimum of two people must be present during all operations.
5. Complete the prestart checkout.
6. (Optional) With the control rods, neutron source, and fission chamber at their lower limits, adjust the discrimination level of the fission chamber system (Channel 1) to a point just above the alpha cutoff level to insure maximum neutron sensitivity.

7. Adjust the discrimination level of the auxiliary system to give the maximum neutron sensitivity without detecting gamma rays or alphas.
8. A fuel loading board with all serial numbers, and dummies should be available and/or in place.

Note: When performing the following steps the statement 'move the rod(s) to the Shim Range (SR)' means move the rod(s) to the lower limit of the SR.

Note: When the following steps are being performed as a part of a known core assembly it will not be a violation on this procedure if it is started at any safe partial loading step. That is to say this procedure may be started part-way through the element list or simply as a plate-by-plate of the last element **H-2**.

Procedure

1. If not previously completed load all required reflector elements into the grid plate.
2. If not previously completed load the source into the source location at **C-3**.
3. Insure that both shim safety (SS) rods are fueled (record the orientation and serial numbers of all fuel placed into the core, also dummy locations as applicable), moving without binding, and at their lower limit (LL) then install the two fueled shim safety rods into the following core locations. SS1 at **G-3** and SS2 at **E-3**.
4. Insure that the regulating rod (RR) is fueled (record the orientation and serial numbers, etc.), moving without binding, and at its lower limit (LL). Install the RR into location **E-5**.
5. If not previously completed install the Fission Chamber (FC) with its associated fuel (record the orientation, serial numbers, locations, and dummies) into location **G-5**.
6. Test raise and lower each rod, the source and the fission chamber check them for binding and insure that the 'Jam' lamp does not come on. Repair as necessary.
7. Complete Procedure M-4 Procedure for Measuring Shim-Safety Rod Drop Times. The drop time is not allowed to exceed 1 second. If the times are much beyond

the normal times (times found in previous drops) recheck the rod for binding. If a rod is found to be binding or scraping on the guard plates this is a good time to repair the problem. The reactor may be secured and any binding or scraping may be examined and/or repaired. Do this now as the core will be hotter after any runs. Note: If the Source, FC, and rods were not previously removed step 7 may be omitted.

8. With the source, FC, and all control rods at their LL, allow time for the count rates to level, take and record the counts on 'Channel-1' and the 'Auxiliary Channel'. These are the initial counts C_0 and should be used as such when calculating graphs [LL-Ch-1] and [LL-AUX], respectively. Note: The first point is plotted as 1.0 vs. total plates loaded on all graphs.
9. Raise all three rods to 50 cm. Again allow time, take and record the counts from 'Channel-1' and the 'Auxiliary Channel' and use as the initial counts C_0 when calculating graphs [50-CH-1] and [50-AUX], respectively.
10. Raise all three rods to their upper limit (UL). Allow time for the count rates to level, take and record the counts from 'Channel-1' and the 'Auxiliary Channel' and use as the initial counts C_0 when calculating graphs [UL-CH-1] and [UL-AUX], respectively.
11. Move the SS rods to the lower limit of their shim range (SR) and the RR to 40cm. This is considered 'cocked'. Allow time for the count rates to level, take and record the counts from 'Channel-1' and the 'Auxiliary Channel' and use as the initial counts C_0 when calculating graphs [Shim-CH-1] and [Shim-AUX], respectively.
12. With the rods still 'Cocked' at the (SR); before installing the element record the fuel orientation, serial numbers, and the locations of any dummies; while observing the instrumentation install element **F-3**.
13. Allow time for the count rates to level, then take counts, calculate C_0/C , and plot as a data point on graphs [Shim-CH-1] and [Shim-AUX] vs. total plates loaded..
14. In each of the following steps allow time for the count rates to level after rod motion. Then take counts; and on their respective graphs, plot the new data points vs. total fuel plate count. Move the rods to the lower limit (LL) take data

and plot it. Plot two graphs [*# of plates* CH-1] and [*# of plates* AUX] 1/M vs. rod height, using (LL) and (SR) data, extrapolate and record the rod height where the reactor will go critical when the rods are raised. If it is predicted that the reactor will not go critical before 50cm then continue with the next step. Else, go to step 28.

15. Watching for critical carefully raise all rods to (50cm) take data and plot [50-CH-1] and [50-AUX]. On the two graphs [*# of plates* CH-1] and [*# of plates* AUX] plot rod height, extrapolate and record where the reactor will go critical via raising the rods. If it is predicted that the reactor will not go critical before the (UL) continue with the next step. Else, go to step 28.

16. Watching for critical carefully raise all rods to the upper limit (UL) take data and plot it on the graphs [UL-CH-1] and [UL-AUX] and [*# of plates*] extrapolate the data estimate and record the banked rod height for criticality, then set both old [*# of plates*] graphs aside.

NOTE: Because these steps are repeated remake two [*# of plates* CH-1] and [*# of plates* AUX] graphs for each fuel addition. Use the more conservative of the two individual graphs to predict the final critical rod height.

17. Using the last two data points on graphs [LL-Ch-1], [LL-AUX], [Shim-CH-1], [Shim-AUX], [50-CH-1], [50-AUX], [UL-CH-1], and [UL-AUX], extrapolate the data to $C_0/C = 0$, predict and record the number of plates required for a critical core loading.

18. If the extrapolated data shows that the next element to be added is less than 50% of the difference between the present core loading and the minimum predicted critical loading, using the most conservative of the two upper limit graphs [UL-CH-1] and [UL-AUX], continue with step 21 and install the next element from the list into the core. If the predicted worth of the next fuel element is greater than 50% of the difference, then a partial loading of the element must be performed, by replacing fuel plates with aluminum dummy plates. If a partial loading of a fuel element must be made, use step 19 and 20. If a whole assembly can be added use step 21 to install the element.

19. Keeping track of serial numbers and orientation, disassemble the fuel element.
{**NOTE:** The removed fuel should be in that part of the element furthest from the center of the core.} Reassemble the element, substituting dummy aluminum plates for any fuel plates that are removed (first pass) adding fuel with each pass. The reassembled element should contain only enough fuel plates to meet the condition of less than 50% of the difference between the present core loading and the predicted minimum critical loading.
20. Repeat the taking of counts and extrapolating as in steps 14 through 21 until the complete element has been safely inserted into the core and a new minimum critical loading determined. If the new determination indicates that the next element can be added under the conditions of step 18, continue with step 21; else repeat step 19 and 20 (with 14-21) for that element.
21. 'Cock the rods' at the shim range (SR) by raising the RR to 40cm and both SS rods to the lower limit of the SR. Record the orientation and serial numbers and install the next element from the list below (i.e. step 22), allow time then take counts and plot on the two graphs [Shim-CH-1] and [Shim-AUX].
22. Repeat steps 14 through 21, for each element. Add elements in the following order: **E-4, F-4, G-4, F-5, G-2, F-2**, (Do step 23) **H-4, H-3, H-5**, and **E-2**.
23. Repeat step 7. Procedure M-4, Procedure for Measuring Shim-Safety Rod Drop Times. (Unless there is any suspected binding {i.e. jam lamp or other indications} step 23 is done only on the first pass. At this point the rods have most of the fuel surrounding them.)
24. Using the last extrapolation on curves [UL-CH-1] and [UL-AUX] and rod height extrapolation from graphs [# of plates CH-1] and [# of plates AUX], determine the minimum number of plates needed in element **H-2** to make the reactor critical with all rods at their upper limit. If element **H-2** becomes filled fuel may be added to any element using steps 24 through 26 and substituting that element number for **H-2**.
25. Dismantle fuel element **H-2**, replacing fuel plates with aluminum dummy plates. Assembled element **H-2** using enough fuel plates to approximate 50% of the

number of plates calculated in step 24. Fuel plate positions should be filled, starting with plates near the center of the core and working away from the core center.

- 26.** Repeat steps 14 through 21 to install the element (Step 21) and also determine a new critical loading.
 - 27.** Repeat steps 24 through 26, adding fuel plates in minimum steps of one plate until the reactor can be made critical.
 - 28.** Operators may at their option complete an approach to critical using subcritical multiplication Procedure #62 or 06-2-IS to find the rod height for banked rods and gain confidence in the new core, or take the reactor critical with a normal startup (Procedure 91-1) at very low power. In either case take the reactor critical, with the regulating rod and SS1 fully withdrawn, level with SS2. Using the last control rod calibration curve, estimate the excess reactivity ρ_{ex} of the core and record this value in the log book. (Also record during iterations.) At some point it will be necessary to find the critical rod positions in the four normal rod configurations; this may be done at this time or at a later date.
 - 29.** For a new core, new control rod, or any time the control rod worths are not known or suspected: use procedures 95-7-RR and 95-7-SS to find the control rod worth curves then complete the following step 30 of adjusting the core excess reactivity.
- Note: After the reactor has been made critical and (for a new core) the rod worths have been determined (the rods calibrated) step 30 (with 24-28) may be used to adjust the core dummy locations. For calibrated rods in an old core use step 30 (with 24-28) for adjustment as above.
- 30.** Repeating steps 24 through 28, adding or removing one fuel plate at a time (dummies may be removed or placed as needed in any element of the core), adjust the excess reactivity of the core to a value between $0.003 \Delta k/k$ and $0.005 \Delta k/k$ with a good fuel and dummy symmetry.
 - 31.** Record the excess reactivity worth of any group or each added plate/s in the log book.
 - 32.** Shutdown the reactor using ganglower.

- 33.** Restore the discriminator on Channel 1 to its normal setting.
- 34.** If no other work is expected, remove the auxiliary detector from the reactor.
- 35.** Secure the reactor.
- 36.** Secure the fuel handling tool.
- 37.** Record the serial numbers and secure any extra plates. Extra plates are allowed to be stored in the pool.
- 38.** If the core has different fuel, a different number of fuel plates, or any dummy plates are moved then change the date on the core loading stamp, stamp or hand write the 'core loading' date on the next few pre-start sheets.

REFERENCES

1. Safety Analysis Report for the Purdue University PUR-1 Reactor, June 30, 1986.
2. Technical Specifications for the Purdue University Reactor, May 1988
3. U.S. Nuclear Regulatory Commission, "Safety Evaluation Report Related to the Renewal of the Operating License for the Research Reactor at Purdue University", NUREG-1283, April 1988.
4. U.S. Nuclear Regulatory Commission, "Safety Evaluation Report Related to the Evaluation of Low-Enriched Uranium Silicide-Aluminum Dispersion Fuel for Use in Non-Power Reactors", NUREG-1313, July 1988.
5. Idaho National Laboratory (INL), "Specification for Purdue University Standard and Control Fuel Elements—Assembled for the Purdue University Reactor," Document ID SPC-382, May 2006.
6. X-5 Monte Carlo Team, "MCNP-A General Monte Carlo N-Particle Transport Code, Version 5 Volume I, II and III," Los Alamos National Laboratory, Report LA-CP-03-0245 (2003)
7. Edward C. Merritt, "Report on Reactor Operations for the Period January 1, 2004 to December 31, 2004". Facility Docket Number 50-182, Purdue University Nuclear Engineering, March 2005
8. R. S. Smith and W. L. Woodruff, "A Computer Code, NATCON, for the Analyses of Steady-State Thermal-Hydraulics and Safety Margins in Plate-Type Research Reactors Cooled by Natural Convection," Argonne National Laboratory (ANL), ANL/RERTR/TM-12, Dec 1988.
9. M. Kalimullah, "NATCON v2.0 Instructions", Argonne National Laboratory (ANL), ANL/RERTR, July 2006.
10. W. L. Woodruff and R. S. Smith, "A Users Guide for the ANL Version of the PARET Code, PARET/ANL (2001 Rev.)," Argonne National Laboratory (ANL), ANL/RERTR/TM-16, March 2001.
11. USNRC, "Guidelines for Preparing and Reviewing Applications for the Licensing of Non-Power Reactors, Format and Content", NUREG 1537, Part 1, Appendix 14.1, February 1996.

This page intentionally left blank.